Nighttime Light and the Construction Financing Channel of Monetary Spillovers*

Kaiji Chen † Qichao Wang‡ Juanyi Xu§ Jingbo Yao¶

Abstract

We identify a financing-based construction channel for the international transmission of U.S. monetary policy. Our design combines high-frequency monetary policy shocks with nighttime light (NTL) big data, providing both the temporal resolution to isolate causal effects and the spatial granularity to trace mechanisms. Using China as a laboratory, we link parcel-level construction activity, measured by NTL, to land transactions and firm-level financing structures. U.S. monetary tightening reduces real activity, with larger effects for firms more exposed to foreign bond financing and tighter balance sheet constraints, and with amplification following the "three red lines" policy. Extending to a global sample, we find stronger spillover effects in emerging markets, consistent with this mechanism.

Keywords: Monetary Policy Spillover, Nighttime Light, Construction Financing Channel.

JEL codes: E44, E52, F30, F42

*We are grateful to Yan Bai, Giacomo Candian, Hui Chen, Zhang Chen, Sangyup Choi, Zhenyu Gao, Kaiji Robin Gong, James D. Hamilton, Rustam Jamilov, Kohei Kawaguchi, Paymon Khorrami, Nobuhiro Kiyotaki, Arvind Krishnamurthy, Byoungchan Lee, Kai Li, Yao Amber Li, Francesco Lippi, Yan Liu, Yang Lu, Peter Maxted, Ryungha Oh, Luigi Paciello, Jun Pan, Benjamin Pugsley, Wei Qiao, Deyu Rao, Isabelle Roland, Harrison Shieh, Zheng (Michael) Song, Vincent Sterk, Eric Swanson, Shang-jin Wei, Jieran Wu, Wenbin Wu, Fan Dora Xia, Wei Xiong, Le Xu, Jianpo Xue, Tony Zhang, Yaoyuan Zhang, Haonan Zhou, Xiaodong Zhu, Yu Zhu, and other participants at the NBER China 2025, 8th Annual Conference on the Chinese Economy (Toronto), the World Congress of Econometric Society, Econometric Society European Winter Meeting, Midwest Macro, CICF, CICM, CFRC, CES China, CES North American, IFABS, China Accounting and Finance Conference, 2nd-HKUST-Fudan-SMU Conference on International Economics, International Conference on The Chinese Economy: Past, Present and Future, EFG, ITDGR, and seminars at BIS, PKU, UIBE, CUFE, CKGSB, HKUST, University of Florida, for helpful comments and suggestions. We especially thank Yi Huang and Xiaoyu Zhang for sharing the bond issuance and land transaction data, respectively.

†Emory University and ABFER. Email:kaiji.chen@emory.edu.

‡The Department of Economics at The Hong Kong University of Science and Technology. Email: qwangcq@connect.ust.hk.

§The Department of Economics at The Hong Kong University of Science and Technology. Email: jennyxu@ust.hk.

¶The Department of Economics at The Hong Kong University of Science and Technology. Email: jyaoam@connect.ust.hk.

1 Introduction

Understanding how U.S. monetary policy transmits internationally to real economic activity remains a central question in macroeconomics. While a large literature documents spillovers to asset prices and capital flows, evidence on real economic consequences and transmission mechanisms remains comparatively limited. A key challenge is empirical identification along two dimensions. First, standard measures of real activity, such as GDP, are observed at quarterly or annual frequency, making it difficult to isolate the causal effects of monetary policy shocks from other forces that co-move over the same horizon. Second, these measures are highly aggregated spatially, which obscures heterogeneity across locations and sectors and makes it difficult to disentangle specific transmission channels—such as construction, consumption, or trade—through which shocks propagate. As a result, both the causal spillover effects and the underlying transmission mechanisms are difficult to identify using traditional data.

This paper attempt to address these challenges by leveraging nighttime light (NTL) data along these two dimensions. First, NTL provides a high-frequency measure of real activity that can be aligned with the timing of monetary policy surprises identified in narrow windows around Federal Open Market Committee (FOMC) announcements. This timing structure helps sharpen identification by reducing the scope for other macroeconomic forces to move systematically with the policy shock within the same window. Second, NTL data can be aggregated at flexible spatial units—from national aggregates down to highly localized geographic cells—under a consistent measurement framework. This spatial granularity makes it possible, when combined with complementary microdata, to connect localized changes in real activity to particular economic agents and sectors, thereby providing new evidence on transmission mechanisms.

Among the sectors most likely to transmit external financial shocks to the real economy, construction is a natural and quantitatively crucial candidate. Construction is highly capital-intensive and requires substantial upfront financing over long investment horizons, making it acutely sensitive to changes in borrowing costs. Crucially, this construction financing channel is not a country-specific phenomenon, but a general and pervasive mechanism across the developing world. In almost all emerging market economies, the construction and real estate sector constitutes a massive share of the real economy—often accounting for 15% to 25% of GDP—and serves as the primary engine of urbanization and growth. As domestic credit markets in these countries often fall short of funding large-scale development, leading developers have increasingly turned to offshore U.S. dollar-denominated bond markets: by the early 2020s, EME real estate firms accounted for nearly 30% of outstanding dollar-denominated high-yield debt globally. This structural shift transforms what is inherently a domestic, non-tradable sector into the direct

frontline of global financial shocks. Traditional international macroeconomics emphasizes trade and exchange rate channels, but these operate primarily through tradable sectors and cannot fully explain why U.S. monetary tightening consistently generates large, synchronized contractions in non-tradable sector. The construction financing channel fills this gap: it traces a direct, balance-sheet-level link between Federal Reserve policy and the investment decisions of firms responsible for the core of emerging market real activity.

China provides an informative setting for studying this mechanism. Construction and real estate together accounted for roughly 25% of GDP over our sample period, making it one of the largest single drivers of aggregate investment. More importantly, China's institutional environment generates sharp, plausibly exogenous variation in firms' exposure to external financing. Following the post-2009 credit expansion, domestic bank lending to real estate developers was progressively curtailed by regulatory tightening, pushing firms toward alternative funding channels. The most consequential of these was the offshore U.S. dollar bond market: by the mid-2010s, Chinese developers had become among the largest issuers of dollar-denominated high-yield debt globally, with outstanding balances reaching roughly 200 billion dollars. This offshore debt is priced directly off U.S. benchmark rates, creating a mechanical and largely unhedged exposure to Federal Reserve policy among firms responsible for a substantial share of China's physical investment. The subsequent introduction of the "three red lines" policy in 2020, which imposed binding leverage constraints on developers and effectively foreclosed domestic borrowing as a margin of adjustment, further sharpened this exposure. The result is a setting where variation in firms' sensitivity to U.S. monetary policy is driven by their financing structure—variation that is both economically large and empirically tractable, enabling us to move beyond documenting average spillover effects and directly identify the channel through which they operate.

We combine high-frequency NTL data with transaction-level land-parcel records and firm-level financial information. Specifically, we construct parcel-level measures of construction activity by mapping satellite pixels to geolocated land transactions and linking each parcel to the corresponding developer. We then merge these data with firms' balance sheets and detailed bond issuance records. The resulting dataset connects the timing and location of construction activity to the identity and financing structure of the firm undertaking each project, allowing us to directly trace how U.S. monetary policy shocks affect firms' financing conditions and how these effects translate into changes in construction activity at the parcel level.

A simple construction-financing framework guides our empirical analysis. When U.S. monetary policy tightens, developers face a deteriorating financing environment; the re-

sulting liquidity squeeze forces them to halt or slow down capital-intensive construction projects, driving a sharp decline in nighttime lights. The transmission of this shock, however, exhibits stark heterogeneity. Although domestic credit constitutes the bulk of developers' debt, cross-border capital controls heavily discount the direct pass-through of U.S. rate hikes to domestic markets. By contrast, developers issuing offshore U.S. dollar bonds leave their balance sheets fully exposed to international financial fluctuations. A corporate pecking-order logic further amplifies this disparity: developers typically exhaust domestic credit quotas first before turning to offshore bonds as a residual financing channel. Consequently, when an external shock hits, the room to adjust along the domestic margin is highly limited. The offshore debt market instead acts as the marginal source of funding with a much larger elasticity of adjustment. Thus, firms with higher reliance on foreign debt should be more affected.

Our empirical results strongly support these predictions. First, U.S. monetary tightening leads to a significant aggregate decline in nighttime lights, an effect heavily concentrated in non-built-up areas characterized by intensive construction activities. Second, this contraction is substantially steeper for projects undertaken by firms with higher overall debt burdens, and specifically those with greater reliance on offshore bond financing. Strikingly, despite accounting for a small share of total debt volume, foreign bond exposure explains the largest share of the variation in NTL responses. Third, exploiting the introduction of China's "Three Red Lines" policy as a quasi-natural experiment, we show that the negative spillover is severely exacerbated for firms forced into tighter domestic liquidity constraints. Fourth, this debt-driven amplification effect remains robust and is even more pronounced in cities with historically strong housing demand. Fifth, aggregating these dynamics to the city level, we construct a "bad deal index" to measure local exposure to financially troubled firms; we find that cities historically more reliant on land sales to highly leveraged developers suffer significantly larger overall declines in construction activity. Together, these results confirm that the transmission operates through a construction financing channel.

Beyond China, we provide suggestive evidence on external validity by extending the analysis to a global sample using aggregate NTL data. We find that the response to U.S. monetary tightening is overall negative and stronger in emerging economies.

Literature and Contribution. This paper contributes to the literature on international monetary spillovers along two dimensions: the identification of causal effects and transmission channels. A large body of work studies the real spillover effects of U.S. monetary policy using low-frequency macroeconomic data and VAR- or FAVAR-based approaches (e.g., S. Kim, 2001, Maćkowiak, 2007, Bluedorn and Bowdler, 2011, Georgiadis,

2016; see Bhattarai and Neely, 2022 for a survey), often complemented by studies emphasizing global financial cycle mechanisms (e.g., Dedola et al., 2017, Miranda-Agrippino and Rey, 2020, Bräuning and Ivashina, 2020). While informative, these approaches rely on low-frequency aggregate outcomes and are subject to concerns about identification restrictions, model misspecification, and contamination from confounding shocks within long observation windows (e.g., Rudebusch, 1998, Miranda-Agrippino and Ricco, 2021). We instead adopt a high-frequency identification strategy that combines monetary policy surprises measured in narrow windows around FOMC announcements—following Gürkaynaka et al., 2005, Nakamura and Steinsson, 2018, Swanson, 2021, and Gürkaynak et al., 2022—with high-frequency measures of real activity from nighttime light (NTL) data. This design tightens the mapping between policy shocks and real outcomes, reducing concerns about omitted variables and reverse causality and thereby delivering sharper causal inference on real spillovers. To our knowledge, we are the first to study the effects of monetary policy on the real economy using nighttime light (NTL) as a high-frequency proxy of real activities.

We also contribute to this literature by identifying a construction-financing channel using spatially disaggregated and micro-linked data. Most existing studies rely on country- or city-level aggregates, where multiple channels—such as trade (Bluedorn and Bowdler, 2011), financial conditions (Bräuning and Ivashina, 2020), and exchange rate movements (Uribe and Yue, 2006)—are jointly embedded, making it difficult to isolate specific mechanisms. We instead exploit the spatial flexibility of NTL data, which can be aggregated from national measures down to sub-city areas and land parcels, and combine it with transaction-level land data and firm-level financing information. This allows us to move beyond documenting average spillover effects and to directly trace a mechanism: U.S. monetary tightening reduces construction activity, particularly for projects undertaken by firms with tighter financing conditions and greater exposure to foreign bond markets, consistent with evidence on corporate external financing channels (e.g., Huang et al., 2024). Documenting this channel is an important contribution in itself. Beyond the inherent importance of the construction sector in emerging economies, this channel helps explain why U.S. tightening often triggers severe contractions in foreign non-tradable sectors, a pattern that traditional trade or exchange rate channels cannot fully account for.

Our paper also relates to the growing literature using NTL data to measure economic activity and provides a general methodological framework to trace macro shock transmission mechanism. Existing studies primarily exploit NTL as a proxy for output at relatively aggregate levels, often at annual or lower frequencies, to study economic growth, development, or broad macroeconomic fluctuations (e.g., Henderson et al., 2012

and Pinkovskiy and Sala-i-Martin, 2016). More recent work has begun to use higher-frequency NTL data to examine specific economic shocks (e.g., Chor and Li, 2024). We build on this literature but depart from it in two important ways. First, we use NTL at a much higher frequency to align with the timing of monetary policy surprises, allowing for sharper causal identification. Second, and more importantly, we exploit its extreme spatial granularity and combine it with transaction- and firm-level data to identify exact economic mechanisms, rather than using NTL solely as an aggregate proxy for economic activities. In this sense, our paper demonstrates a broader methodological framework: by isolating high-frequency NTL at specific functional locations and linking them to micro-level data, researchers can pinpoint the precise transmission channels of a wide array of aggregate shocks. For instance, just as we leverage geo-coded land parcels to identify the real estate construction channel, this approach can be readily generalized to other contexts—such as utilizing NTL at port facilities to trace international trade channels, or isolating lights at specific factory coordinates to investigate manufacturing responses. Ultimately, we highlight that spatially disaggregated NTL data, when paired with complementary micro-datasets, serves as a highly adaptable and powerful tool for mapping virtually any macroeconomic shock to localized, sector-specific real economic outcomes.

The remainder of the paper proceeds as follows. Section 2 describes the data. Section 3 presents baseline empirical results. Section 4 identifies the financing channel and quantifies its importance. Section 5 examines external validity using cross-country evidence. Section 6 concludes.

2 Data and Measurement

This section describes the data and the construction of our integrated dataset. Our empirical design combines three key elements: (i) high-frequency U.S. monetary policy shocks, (ii) high-frequency measures of real activity from nighttime light (NTL) data, and (iii) micro-level data linking construction activity to firms' financing conditions. This combination allows us to study how U.S. monetary policy shocks transmit to real activity and to identify the role of external financing in this transmission. Detailed data construction and validation are provided in Appendix A.

2.1 U.S. Monetary Policy Shocks

Our baseline monetary policy shock is constructed from high-frequency changes in federal funds futures prices around Federal Open Market Committee (FOMC) announcements,

following Gürkaynaka et al. (2005).[1] These shocks capture unexpected changes in monetary policy within narrow time windows and are widely used in the literature to identify exogenous policy surprises.

We focus on the period from 2012 to 2023, during which 95 scheduled FOMC meetings took place. The timing of these shocks provides sharp variation that can be aligned with high-frequency measures of real activity. In robustness checks in the Appendix, we also consider alternative measures of monetary policy shocks, including unconventional policy shocks and shocks from other central banks.

2.2 Nighttime Light Data

We use nighttime light (NTL) data from NASA's Black Marble product, available at daily frequency from 2012 onward. These data provide a high-frequency proxy for real economic activity and can be aggregated at flexible spatial units, ranging from national aggregates to highly localized geographic cells.

For our analysis, we aggregate daily NTL data to the weekly frequency to align with the timing of monetary policy shocks while reducing measurement noise. At this frequency, NTL provides a timely measure of changes in real activity that can be directly linked to policy shocks identified in narrow event windows.

To facilitate empirical analysis, we construct city-level NTL series for 345 prefecture-level cities in mainland China. In addition, the spatial granularity of the data allows us to measure activity at sub-city areas and at specific land parcels, which is central to identifying the construction channel studied in this paper.

Consistent with existing literature, NTL is strongly correlated with traditional measures of economic activity such as GDP. We provide additional validation in Appendix B.

2.3 Land Transaction Data

To study construction activity at a granular level, we use transaction-level land data from Land China (www.landchina.com). These data record the location, timing, and characteristics of land parcels purchased by real estate developers.

We geolocate each transaction and manually match it to the corresponding NTL cell, allowing us to construct parcel-level measures of construction activity. We further match

[1]The data are obtained from Jarociński (2024). We also use the shock of Acosta (2022) as a robustness check.

each land parcel to the associated listed real estate firm. This linkage is a key feature of our dataset, as it connects localized economic activity to firm-level characteristics.

2.4 Bond Issuance and Firm-Level Data

To measure firms' exposure to external financing, we use bond issuance data from Huang et al. (2024), which provide detailed information on issuance amounts and currency denomination. These data allow us to distinguish between domestic and foreign bond financing.

We combine these data with firm-level balance sheet information, including leverage, liabilities, and other financial indicators. This enables us to characterize firms' financing structures and to measure their exposure to external funding conditions.

2.5 Integrated Dataset

Our final dataset links three layers of information: (i) the timing and location of construction activity, measured using NTL at the parcel level; (ii) the identity of the firm undertaking each project; and (iii) the firm's financing structure, including exposure to foreign bond markets.

This integrated structure allows us to move beyond aggregate correlations and to directly connect localized real activity to firm-level financing conditions. In particular, it enables us to trace how monetary policy shocks affect firms' financing costs and how these effects translate into construction activity at specific locations.

In the next section, we use this dataset to establish the real effects of U.S. monetary policy shocks and to identify the margin of adjustment. Section 4 then builds on this same empirical design to identify the underlying transmission mechanism.

3 Spillover Effects of U.S. Monetary Policy Shocks

We begin by using the integrated dataset described in Section 2 to estimate the real effects of U.S. monetary policy shocks. The combination of high-frequency shocks and spatially disaggregated nighttime light (NTL) data allows us to isolate causal effects while identifying the margin along which real activity adjusts.

This section establishes two empirical facts that guide the subsequent mechanism analysis. First, U.S. monetary tightening reduces real economic activity in China, as measured by nighttime light (NTL). Second, the contraction is concentrated in areas

associated with construction activity. Together, these findings motivate the focus on the construction margin and the financing channel analyzed in Section 4.

3.1 Empirical Specification

We estimate the dynamic effects of U.S. monetary policy shocks using local projections (Jordà, 2005) at the weekly frequency. The high-frequency design aligns policy shocks with real activity measured over short windows, reducing contamination from other macroeconomic forces.

Our baseline specification is:

$$y_{t+h} - y_{t-1} = \alpha^{(h)} + \sum_{q=1}^{Q} \phi_q^{(h)} \Delta y_{t-q} + \beta^{(h)} x_t + \gamma^{(h)} W + u_{t+h|t}, \tag{1}$$

where y_t denotes log NTL in week t, x_t is the high-frequency monetary policy shock around FOMC announcements, and W represents additional controls. We select lag lengths using the AIC criterion and results are robust to using BIC. The coefficients $\{\beta^{(h)}\}_{h=0}^{H}$ trace out the impulse response function (IRF). We report responses up to $H = 20$ weeks.

The identification assumption is that, within narrow windows around FOMC announcements, monetary policy shocks are orthogonal to other shocks affecting real activity.

3.2 Aggregate Effects

Figure 1 presents the baseline impulse responses. U.S. monetary tightening leads to a statistically significant decline in NTL, indicating a contraction in real activity.

Two features are notable. First, the response is economically meaningful: a one-standard-deviation tightening shock reduces NTL by approximately 1.92 percents over a 20-week horizon. Using the empirical elasticity between NTL and GDP (0.49), this corresponds to roughly a 0.8 percent decline in output. Results are robust to a wide range of tests, see Appendix C. Second, the response materializes quickly, within a few weeks of the policy shock, suggesting a relatively rapid transmission mechanism.

Appendix F further examines alternative monetary policy shocks and transmission channels. We find that the baseline results are primarily driven by conventional U.S. monetary policy shocks, while unconventional shocks and shocks from other major economies yield weaker or insignificant effects.[2]

[2]In addition, trade exposure tends to attenuate the response of nighttime light, but it is not the dominant transmission channel.

These findings are consistent with the broader literature on international monetary spillovers, but are identified here using a much tighter event window and higher-frequency outcome measure.

3.3 Heterogeneity across Subareas Within a City

We next examine the spatial distribution of the response to identify the underlying margin of adjustment. We decompose each city into three areas: (i) city centers, (ii) suburbs, and (iii) non-built-up areas. These areas are mainly characterized by service activity, manufacturing activity, and construction activity, respectively. The classification is based on historical built-up boundaries derived from satellite data.

For each city, we identify the built-up areas in different years using the boundary of satellite images (Jiang et al., 2022). We exclude uninhabitable lands defined by the land cover map from the China Land Cover Dataset (CLCD). The percentage of built-up area identified by the geospatial data is positively correlated with the urban constructed rate from NBSC, as shown in Appendix B. We define the city center as the area built in 1990, the suburb as the area built up in 2010 but not in 1990, and the non-built area as other parts.[3] We choose 2010 as the threshold year because the NTL series starts from 2012, therefore excluding potential endogeneity issues.[4] We illustrate the division of the city center, the suburb, and the non-built-up area for selected cities in Figure A.3.

Figure 2 shows the heterogeneous responses across areas. The decline in NTL is almost entirely driven by non-built-up areas, while responses in city centers and suburbs are small and statistically insignificant. The NTL in non-built-up areas mainly reflects the real activities of construction, such as the light from construction sites at night and from new buildings. This pattern indicates that the aggregate contraction in NTL primarily reflects a reduction in construction activity rather than broad-based declines across sectors. The results suggest that investment in construction is one of the key margins through which U.S. monetary policy affects real activity.

The concentration of the response in construction-related areas points to a specific margin of adjustment: investment in construction. Given the reliance of construction activity on external financing, this pattern suggests a financing-based transmission mechanism.

In the next section, we test this mechanism directly by linking parcel-level construction activity to firm-level financing conditions and examining how variation in financing

[3] We validate this classification using major cities.

[4] Results are robust to alternative cutoff years (see Appendix C).

exposure shapes the response to U.S. monetary policy.

4 Identifying the Construction-Financing Channel

Section 3 shows that U.S. monetary tightening reduces real activity and that the contraction is concentrated in construction-related areas. This section uses the same empirical design—linking parcel-level activity to firm-level data—to identify the mechanism underlying this decline.

Our approach leverages the integrated dataset constructed in Section 2, which connects three layers: construction activity at the parcel level, the identity of the developer, and the firm's financing structure. This linkage allows us to trace how monetary policy shocks affect financing conditions and how these effects propagate to real investment.

The empirical analysis proceeds in five steps. First, we establish that construction activity declines at the parcel level. Second, we show that U.S. monetary tightening directly deteriorates firms' financing conditions. Third, we document that firms with weaker balance sheets exhibit larger declines in construction activity, and that this heterogeneity is driven primarily by exposure to foreign bond financing. Fourth, we quantify the aggregate importance of this financing channel. Fifth, we exploit the "three red lines" policy as a quasi-natural experiment and use parcel-level variation to sharpen identification and rule out alternative demand-side explanations.

Taken together, the evidence provides a coherent interpretation of the findings in Section 3. U.S. monetary policy affects real activity primarily through a construction-financing channel operating via firms' external financing costs.

4.1 Average Effects of U.S. Monetary Spillover on Construction Activity

We begin by focusing directly on construction activity using nighttime light (NTL) measured at land parcels developed by real estate firms. These parcels correspond closely to construction sites: approximately 86 percent of geolocated transactions occur in non-built-up areas.[5]

For each land parcel that we can associate with a listed real estate firm, we geolocate its coordinates by reverse geocoding the textual address. We then match each parcel to

[5]Among the 265 cities with geolocated land transactions, only 54 have less than 80 percent of the lands in the non-built-up area, and only 12 have less than 60 percent of the lands in the non-built-up area.

the corresponding NTL grid cell, using the cell's nighttime light intensity as a proxy for construction activity at that site. Aggregating across all parcels linked to listed firms, we estimate the response using the baseline local projection specification.

Figure 3 shows that NTL at these parcels declines significantly following U.S. monetary tightening. This is consistent with our baseline, which implies that the response of the construction works is a driver of the overall decrease in NTL. The magnitude of the response at the parcel level is comparable to the aggregate response, indicating that construction-related activity accounts for a substantial share of the overall decline in NTL. This suggests that the contraction in real activity documented in Section 3 is not diffused across sectors but is concentrated in investment-intensive activities associated with land development.

These findings establish that construction activity is a key margin through which U.S. monetary policy affects real activity. We next turn to the mechanism behind this decline by examining how monetary policy shocks affect firms' financing conditions and how these effects propagate to construction activity.

4.2 Financing Conditions and Construction Activity

We now examine whether the decline in construction activity is driven by deteriorating financing conditions. The analysis proceeds in two steps. We first establish that U.S. monetary tightening worsens firms' financing conditions (first stage). We then show that these financing shocks translate into heterogeneous responses in construction activity, depending on firms' balance sheet strength (second stage). Finally, we decompose the channel by debt type to identify the primary transmission margin.

4.2.1 First-Stage Effects: Impacts on External Financing

We next examine the impact of U.S. monetary policy shocks on firms' financing conditions. Using firm-level bond issuance data from Huang et al. (2024), we explore whether U.S. MP tightening has a negative impact on bond issuance by real estate firms. The specification is as follows.

$$\left(\frac{\text{Net Bond Value Standing Value}}{\text{Operation Indicator}}\right)_{i,t} = \beta_1 x_t + \alpha_i + \varepsilon_{i,t}. \tag{2}$$

Here i is firm, t is month, x_t is the monetary policy surprise, and α_i is the firm FE. The point estimate to look at is β_1. We scale net standing value of a firm's bonds by its size, as represented by asset, liability, current liability, or long-term liability.

We find that the U.S. tightening significantly impedes foreign bond financing of real estate firms, especially with regard to short-term debt (Table 1 Panel A), while the

domestic bond financing is not significantly impeded (Table 1 Panel B). Using a same specification, it is also found that firms' interest expenses significantly increase after a tightening shock, indicating a bigger debt burden (Table 2). These results provide direct evidence on the first stage of the transmission mechanism: U.S. monetary policy shocks tighten external financing conditions faced by firms.

The reduction in foreign bond issuance provides direct evidence on the first stage of the transmission mechanism. Quantitatively, U.S. monetary tightening reduces firms' access to external financing and increases their debt servicing burden, which in turn constrains their ability to undertake new construction projects or continue existing ones. The absence of a comparable effect on domestic bond financing is consistent with the institutional features of China's financial system, where credit allocation is largely quantity-based.

These results establish the first stage of the transmission mechanism: U.S. monetary tightening directly constrains firms' external financing and increases debt servicing burdens. We next examine how this financing shock translates into real activity.

4.2.2 Heterogenenous Responses of NTLs by Financing Conditions

We now turn to the second stage of the mechanism by examining whether firms with weaker balance sheets exhibit stronger responses in construction activity.

To identify the role of financing conditions, we first examine whether firms with a higher debt burden are more sensitive to U.S. monetary tightening by looking at the NTL change of the lands purchased by real estate firms. The specification is

$$y_{i,t+h} - y_{i,t-1} = \alpha_i^{(h)} + \sum_{q=1}^{4} \phi_q^{(h)} \Delta y_{i,t-q} + \beta_1^{(h)} x_t + \beta_2^{(h)} x_t s_{i,t-L} + \beta_3^{(h)} s_{i,t-L} + \gamma^{(h)} W_{i,t-L} + u_{i,t+h|t}. \tag{3}$$

Here $s_{i,t-L}$ is the dummy of firm i's debt ratio in the last quarter, denoted by the lag operator L, to exclude potential endogeneity issues. The control variables in $W_{i,t-L}$ include the lagged asset and profit ratio of the firm, and their interaction terms with MPs. $\alpha_i^{(h)}$ denotes firm fixed effect. We classify a firm as having "High Debt Ratio" if the firm has a debt ratio higher than the median of all firms in a given quarter. The baseline effect β_1 is statistically indistinguishable from zero across almost all horizons. This implies that for firms with debt ratios below the median, the US monetary policy shock has weak impact on their NTL. The coefficients of monetary shock $\beta_1^{(h)}$ and the interaction term of U.S. MPs and the debt ratio dummy $\beta_2^{(h)}$ are shown in Figure 4. It is overall negative, which indicates that the NTL of a firm with a higher debt ratio is more impacted by the U.S. tightening.[6]

[6]Results are robust to control time fixed effect to include any time-varying common factors. In this

The evidence above shows that financially weaker firms respond more strongly to monetary tightening. We next ask which components of firms' financing structures drive this heterogeneity.

4.2.3 Role of Debt Categories

We would like to further identify the specific financing vehicles through which U.S. monetary tightening affects the construction activities by real estate firms. A real estate firm's overall debt consists mainly of domestic loans, domestic bonds and Foreign bonds. A U.S. monetary tightening would lead to an increase in interest payment for all these debt categories via different markets. To assess the importance of individual debt categories for the spillovers, we use the following specification.

$$y_{i,t+h} - y_{i,t-1} = \alpha_i^{(h)} + \sum_{q=1}^{4} \phi_q^{(h)} \Delta y_{i,t-q} + \beta_1^{(h)} x_t + \beta_{FB}^{(h)} x_t s_{i,t-L}^{FB} + \beta_{DB}^{(h)} x_t s_{i,t-L}^{DB} + \beta_{DL}^{(h)} x_t s_{i,t-L}^{DL} + \beta_4^{(h)} s_{i,t-L}^{FB} + \beta_5^{(h)} s_{i,t-L}^{DB} + \beta_6^{(h)} s_{i,t-L}^{DL} + \gamma^{(h)} W_{i,t-L} + u_{i,t+h|t} \tag{4}$$

Here $s_{i,t-L}^{FB}$, $s_{i,t-L}^{DB}$, and $s_{i,t-L}^{DL}$ represent the ratios of foreign bonds, domestic bonds, and domestic loans to total assets in the last quarter, respectively. These variables are transformed into dummy indicators that equal 1 if the respective ratio is above the median for that category in a given period. $W_{i,t-L}$ contains all the additional control variables, including the lagged asset and profit ratio of the firm, and their interaction terms with MPs. The IRFs of β_1, β_{FB}, β_{DB}, and β_{DL} are displayed in Figure 5, respectively.

The top right panel shows that firms with greater foreign bond exposure experience significantly more negative responses to U.S. monetary tightening, with β_{FB} becoming significantly negative from around week 6 onward. This indicates that offshore debt is a key source of vulnerability. The coefficient on domestic loans (β_{DL}) is also negative, suggesting some additional sensitivity for firms with higher loan exposure, though the statistical significance is considerably weaker than that of foreign bonds. By contrast, the coefficient on domestic bonds (β_{DB}) is statistically indistinguishable from zero across most horizons, indicating that domestic bond financing does not amplify the transmission of U.S. monetary shocks. [7] This suggests that U.S. monetary tightening affects negatively the construction activities mainly through an increase in the financing cost of foreign bonds.

case, the level effect of monetary policy β_1 is absorbed.

[7] After around 12 weeks, the coefficient of domestic bond is slightly positive, which seems to indicate that firms issuing more domestic bonds experience a weaker effect. This is plausible because firms may issue more domestic bonds to offset the financing limitation originating from foreign adverse shocks.

The decomposition by debt type further clarifies the mechanism. The stronger response for firms with higher foreign bond exposure indicates that the transmission of U.S. monetary policy operates primarily through external financing costs, rather than domestic credit conditions. This is consistent with the global financial cycle view, in which U.S. monetary policy directly affects the cost of dollar-denominated financing.

4.3 Quantifying the Financing Channel

The preceding results establish that financing conditions are central to the transmission mechanism. We now quantify the importance of this channel and assess which components of firm financing drive the aggregate response.

We begin by decomposing the overall effect into a baseline component and a financing-driven component. We then further decompose the financing channel by debt type to evaluate the relative contributions of foreign bonds, domestic bonds, and bank loans.

4.3.1 The Contribution of Financing Channel

Framework. Our empirical specification implies that the response of construction activity at the parcel (or firm) level can be written as:

$$\Delta y_{i,t+h} = \beta_1^{(h)} + \beta_2^{(h)} s_i, \tag{5}$$

where s_i is firm i's exposure to external financing (e.g., debt ratio or foreign bond dependence), $\beta_1^{(h)}$ captures the average effect, and $\beta_2^{(h)}$ captures amplification through the financing channel.

Aggregating across firms using weights ω_i (e.g., based on land transaction value), the aggregate response can be written as:

$$\Delta Y_{t+h} = \beta_1^{(h)} + \beta_2^{(h)} \bar{s}, \tag{6}$$

where $\bar{s} = \sum_i \omega_i s_i$ denotes the average exposure in the economy.

Decomposition. This expression allows us to decompose the aggregate response into two components:

$$\Delta Y_{t+h} = \underbrace{\beta_1^{(h)}}_{\text{Baseline Effect}} + \underbrace{\beta_2^{(h)} \bar{s}}_{\text{Financing Channel}}. \tag{7}$$

The second term captures the portion of the aggregate decline attributable to the financing channel. We define the share of the total effect explained by financing as:

$$\text{Share}_{\text{finance}}^{(h)} = \frac{\beta_2^{(h)} \bar{s}}{\beta_1^{(h)} + \beta_2^{(h)} \bar{s}}. \tag{8}$$

Empirical Implementation. We implement this decomposition using the estimated coefficients from Equation 3 without control of other firm-specific variables $W_{i,t-L}$. We construct the variable $\bar{s}$ as a weighted average, using the land transaction value of each firm as the respective weights.

Overall, the decomposition highlights that the financing channel is not only a statistically detectable mechanism but also a quantitatively central driver of the real effects of international monetary spillovers. The baseline effect ($\beta_1^{(h)}$) is statistically indistinguishable from zero across all horizons. This implies that for firms with debt ratios below the median, the U.S. monetary policy shock has *almost no impact* on their NTL. MPS *only* exerts a significant negative effect on highly leveraged firms.

4.3.2 Decomposition of Different Debt Components

Having established that the financing channel drives the entirety of the aggregate decline, we now explore which type of debt—foreign bonds (FB), domestic bonds (DB), or domestic loans (DL)—is more important quantitatively in transmitting U.S. monetary policy shocks through the financing channel. To answer this question, we calculate their relative shares.

Method 1: Coefficient-Based Decomposition.

Framework. The empirical specification Equation 4 in Section 4.2 helps to assess the importance of individual debt categories for the spillovers of US monetary policy on firm/parcel level NTL. It implies that the total response of construction activity at the parcel (or firm) level can be written as the sum of the baseline effect and the additional effects from each debt component, scaled by their respective weighted averages:

$$\Delta y_{i,t+h} = \bar{\beta}_1^{(h)} + \bar{\beta}_{FB}^{(h)} \cdot \bar{s}_{FB} + \bar{\beta}_{DB}^{(h)} \cdot \bar{s}_{DB} + \bar{\beta}_{DL}^{(h)} \cdot \bar{s}_{DL} \tag{9}$$

where $\bar{s}_X$ represents the weighted average of each component. The relative share of each component within the financing channel is then given by:

$$\text{Share}^{(X)} = \frac{\bar{\beta}_X^{(h)} \cdot \bar{s}_X}{\bar{\beta}_{FB}^{(h)} \cdot \bar{s}_{FB} + \bar{\beta}_{DB}^{(h)} \cdot \bar{s}_{DB} + \bar{\beta}_{DL}^{(h)} \cdot \bar{s}_{DL}} \quad \text{for } X \in \{FB, DB, DL\} \tag{10}$$

We compute the relative contribution of each debt component using the estimated coefficients, adjusted for statistical significance. Specifically, we set the coefficient to zero

at any horizon where the estimate is not statistically significant at the 90% confidence level, and then average across horizons $h = 0$ to 20. The significance-adjusted average coefficients are $\bar{\beta}^{(h)}_{\text{FB}} = -0.3679$, $\bar{\beta}^{(h)}_{\text{DB}} = 0.0000$ (insignificant at all horizons), and $\bar{\beta}^{(h)}_{\text{DL}} = -0.0688$. Combined with the revenue-weighted averages of the indicator variables ($\bar{s}_{FB} = 0.1885$, $\bar{s}_{FB} = 0.6360$, $\bar{s}_{FB} = 0.7651$), the relative shares within the financing channel are 56.89%, 00.00%, and 43.11%, respectively.

Obviously, foreign bonds account for the majority of the negative impact on construction activity through the financing channel, followed by domestic loan (43.11%). Notably, Domestic Bonds contribute nothing to the financing channel after adjusting for statistical significance—their average estimated coefficients are indistinguishable from zero across horizons. This is particularly striking given that foreign bonds only represent a relatively small share of the total interest-bearing debt of RE firms, 6% on average, while the shares for domestic bonds and domestic loans are 6% and 65% respectively.[8] Despite their small share in total debt, Foreign Bonds exert a disproportionately large effect on the transmission of U.S. monetary policy shocks. This further confirms the dominant role of offshore debt exposure in the transmission of the monetary policy shock.

Method 2: Variance Decomposition (Shapley Value R^2 Approach). As a complementary exercise, we also decompose the within-R^2 of the regression model using the Shapley value approach, which provides an objective, order-independent measure of how much variance in the construction activity (NTL) is attributable to each debt component's interaction with the monetary policy shock.[9]

Consistent with the coefficient-based decomposition, the variance-based approach confirms that foreign bonds are the dominant driver of the financing channel, explaining 66.10% of the variation attributable to debt-component interactions. Despite domestic loans and Domestic Bonds accounting for a much larger share of total debt volume, their contributions to the monetary policy-induced financing constraints are relatively minor (17.87% and 16.03%, respectively).

Both decomposition methods point to the same conclusion: foreign bonds are the most important debt component in transmitting U.S. monetary policy shocks to Chinese real estate construction activity. This finding is economically intuitive—offshore USD-

[8]Other forms of debt account for 23%. In the Chinese real estate sector, developers heavily rely on shadow banking credits (such as trust loans and asset management plans), supply chain financing (e.g., interest-bearing commercial acceptances), and off-balance-sheet financing. However, accurate data for these opaque channels are typically unavailable. We rely on the aforementioned three primary components, which robustly proxy the firm's core formal financing constraints in standard capital markets.

[9]The Shapley value decomposition averages each variable's marginal contribution to the model R^2 over all possible orderings in which variables can be added, thereby resolving ambiguities arising from multicollinearity. See Appendix E for details.

denominated bonds are directly exposed to U.S. interest rate movements, creating a tight mechanical link between Federal Reserve tightening and the financing costs of Chinese developers with foreign bond obligations. In contrast, domestic debt instruments are more insulated from external rate shocks, and their contribution to the financing channel is correspondingly smaller. These results reinforce the interpretation that the international monetary policy spillover operates primarily through the structural vulnerability created by external financing, especially offshore dollar debt exposure.

To summarize, the decomposition yields a clear conclusion. The baseline effect is statistically negligible, indicating that U.S. monetary policy has little impact on firms with low leverage. Instead, the entire aggregate decline is driven by firms with high exposure to external financing. Moreover, despite representing a small share of total debt, foreign bonds account for the majority of the financing channel, highlighting the disproportionate role of offshore debt in transmitting U.S. monetary shocks.

4.4 Quasi-Natural Experiment: The Three-Red-Line Policy

We further strengthen identification using the introduction of the "three red lines" policy as a quasi-natural experiment. This policy imposes binding leverage constraints on real estate developers and generates exogenous variation in firms' access to domestic financing.

The key idea is straightforward: if the financing channel is central, then firms whose domestic financing margins are constrained by the policy should become more sensitive to U.S. monetary shocks.

The "Three-red-line" policy was introduced by the People's Bank of China (PBC), the China Banking and Insurance Regulatory Commission, and other governmental institutions in China to control the overwhelming debt of real estate firms to prevent potential financial risk. It was implemented on August 20th, 2020. The three red lines of real estate companies are measured as follows: (1) $\frac{\text{Liability}-\text{Presales Revenue}}{\text{Asset}-\text{Presales Revenue}}$; (2) $\frac{\text{Interest-bearing Liability}-\text{Cash}}{\text{Equity}}$; (3) $\frac{\text{Cash}}{\text{Short-term or Maturing Interest-bearing Liability}}$. For the first two indicators, the acceptable upper limit is 0.7 and 1, respectively. For the third indicator, the acceptable lower limit is 1. Those cross-line firms will experience harsher financing restrictions under this policy. Therefore, to examine the role of financing conditions, we expect that for those firms violating the red lines, compared with those not-violating firms, the responses of NTLs to U.S. MPs would be more negative after the three-red-line policy was implemented.

The specification is as follows:

$$\begin{aligned} y_{i,t+h} - y_{i,t-1} =& \alpha_i^{(h)} + \alpha_t^{(h)} + \sum_{q=1}^{4} \phi_q^{(h)} \Delta y_{i,t-q} + \beta_j^{(h)} x_t \cdot Policy_t \cdot Cross_i^j \\ &+ \gamma_j^{(h)} x_t \cdot Cross_i^j + \delta_j^{(h)} Policy_t \cdot Cross_i^j + \theta_j^{(h)} W_{i,t-L} + u_{i,t+h|t} \end{aligned} \tag{11}$$

where $Policy_t$ is a time dummy, which equals 1 if after the implementation of policy and 0 otherwise, $Cross_i^j$ is a time-invariant dummy variable that equals 1 if firm i breached red line j in 2019, right before the assessment period, and $W_{i,t-L}$ is similar to the one in Equation 3.

Figure 6 displays γ_h and β_h associated with the third line, the short-term debt constraint (cash-to-short-term debt ratio below 1). The coefficient γ_h is overall positive, indicating that before the implementation of the Three Red Line policy, firms that had already breached this threshold were less affected by U.S. monetary tightening. This pattern is economically intuitive: firms violating the short-term debt constraint prior to 2020 tend to be the largest and most established developers (e.g., Evergrande), which at that time still enjoyed ample access to domestic financing channels—including bank loans and domestic bond markets. Their ability to substitute toward domestic funding sources effectively insulated them from fluctuations in offshore borrowing costs, dampening the negative spillover of U.S. monetary shocks.

By contrast, β_h is significantly negative, indicating a sharp reversal after the policy's implementation. Once the three red lines were imposed, these firms' domestic borrowing capacity was effectively exhausted. Following a pecking-order logic, domestic credit channels were no longer an available margin of adjustment under stress, forcing these developers to rely more heavily on offshore USD-denominated debt as a residual source of financing, precisely the channel most directly exposed to U.S. interest rate movements. The result is a dramatic amplification: after the policy, U.S. monetary tightening transmits far more strongly to the construction activities of these financially constrained developers, as their remaining financing margin is the one most sensitive to U.S. monetary tightening. As a robustness check, we also estimate a subsample regression to examine the heterogeneity across periods. As shown in Figure D.1, in the pre policy period, those firms with a low cash ratio are less affected, while this effect is greater after the policy.

This pattern provides further compelling evidence that the binding nature of financing constraints—not merely the level of leverage—determines the strength of international monetary transmission. When domestic alternatives are available, firms can absorb external rate shocks with limited real consequences; when those alternatives are foreclosed by regulatory policy, the financing channel becomes the dominant mechanism through which U.S. monetary tightening depresses real activity.

We also show the coefficients of the triple interaction term $\beta_j^{(h)}$ regarding other red lines in Figure D.2 . The coefficients for the other two constraints, the liability-to-asset ratio and the net gearing ratio, are less significant. This suggests the decline in NTL is mainly driven by a liquid shortage in the short run.

In addition to the triple-interaction model, our subsample estimations in Figure D.3 reveal the heterogeneous impact of the policy for each group of firms separately. Post-implementation, U.S. tightening exerts a significantly sharper drag on the construction activities of short-debt-constrained firms. While unconstrained firms also exhibit slightly heightened sensitivity, the effect is notably weaker. This divergence indicates that stringent financial constraints act as a powerful amplifier, increasing the exposure of real activities to external monetary shocks.

To summarize, we find that prior to the policy, firms breaching the constraints are less sensitive to U.S. monetary shocks, consistent with their continued access to domestic financing. After the policy, the pattern reverses sharply: these firms exhibit significantly larger declines in construction activity following U.S. monetary tightening.

This reversal reflects a shift in the marginal financing channel. Once domestic borrowing capacity is constrained, firms rely more heavily on offshore financing, which is directly exposed to U.S. interest rates. As a result, external shocks transmit more strongly to real activity. This evidence highlights that the binding nature of financing constraints—not just leverage levels—determines the strength of monetary spillovers.

4.5 Parcel-Level Evidence and Demand-Side Considerations

The firm-level results so far establish a financing channel by aggregating NTL across all parcels linked to each developer. In this section, we sharpen identification by moving to the individual land parcel as the unit of analysis. Conducting the analysis at the parcel level offers several advantages. First, it allows us to include parcel fixed effects and, crucially, city-by-week fixed effects that fully absorb all time-varying local macroeconomic conditions—such as regional policy interventions or local credit cycles. The remaining variation isolates how construction activity at parcels within the same city and the same week responds differentially depending on the financing exposure of the parent firm, providing a substantially sharper test of the financing channel than firm- or city-level regressions can offer. Second, NTL measured at the parcel level captures construction intensity directly at the project site, offering a cleaner mapping from monetary shocks to real activity than firm-level aggregates, which combine multiple projects across different locations. Third, the spatial granularity of parcel-level data is essential for linking firm-level financing conditions to city-specific factors, enabling interaction tests that would be

infeasible at higher levels of aggregation.

We estimate the following specification at the parcel level:

$$\begin{aligned}\Delta_h \log(NTL_{i,t+h}) =& \alpha_i + \gamma_t + \beta^{(h)}(MPS_t \times HighDebt_{j,t-1}) \\ &+ \delta HighDebt_{j,t-1} + \sum_{p=1}^{4} \phi_p \Delta \log(NTL_{i,t-p}) + \epsilon_{i,t+h}\end{aligned} \tag{12}$$

Specifically, the dependent variable $\Delta_h \log(NTL_{i,t+h})$ is the cumulative change in the log of parcel-level nighttime lights from week $t-1$ to $t+h$. MPS_t is the high-frequency U.S. monetary policy shock. $HighDebt_{j,t-1}$ is a binary indicator equal to one if the liability-to-asset ratio of parcel i's parent firm in the previous quarter exceeds the sample median. α_i and γ_t denote parcel and week fixed effects, respectively (note that the main effect of MPS_t is absorbed by γ_t).

Results are consistent with those at the-firm level estimation in Section 4.2.2, see Panel (a) of Figure 7. The figure shows that NTL at land parcels purchased by firms with higher debt ratios responds more negatively to U.S. monetary tightening, confirming that the financing channel operates at the level of individual construction sites.[10] Results are robust if we additionally control firm asset and profit ratio as well as their interaction terms with monetary surprise, see Panel (b) of Figure 7.

A natural alternative explanation is that U.S. monetary tightening reduces construction through lower housing demand rather than tighter financing conditions. The parcel-level framework allows us to test this directly. We find that controlling for local housing demand does not attenuate the estimated effects, indicating that the contraction is not driven by demand alone.

We augment Equation 12 by additionally controlling for housing demand in the city where the parcel is located—measured by floor space sold per capita. As shown in Panel (c) Figure 7, the interaction term between the U.S. monetary shock and the developer's debt ratio remains highly significant. This confirms that the observed contraction in construction activity is primarily driven by the firm-level financing channel rather than a localized demand-side slump. These results hold robustly even when we absorb unobserved local shocks using city-by-week fixed effects, see Panel (d) of Figure 7.

[10]We exclude the 2020–2022 period from the parcel-level regressions to rule out confounding effects from China's 'Dynamic Zero-COVID' policy. The region-specific, unpredictable lockdowns during this period mechanically disrupted local construction activities, which would systematically distort the NTL responses to U.S. monetary policy shocks and introduce significant estimation bias.

Having established that the financing channel—not local demand—drives the baseline contraction, a natural follow-up question is how local housing market conditions interact with the financing mechanism to influence the monetary spillovers. The direction is a priori ambiguous. On the one hand, cities with stronger housing demand generate larger pre-sale revenues, which could mitigate the financing channel by providing developers with internal cash flow to buffer external financing shocks. On the other hand, if U.S. monetary tightening depresses housing sales, the resulting loss of pre-sale revenues could amplify the financing channel, particularly for highly indebted developers who depend on these inflows to service existing debt and sustain construction. To discriminate between these two possibilities, we estimate a triple interaction framework, as specified in Equation 13:

$$\begin{aligned}\Delta_h \log(\mathrm{NTL}_{i,t+h}) = \alpha_i + \eta_{c,t} + \beta_1^{(h)}(x_t \times \mathrm{HighDebt}_{j,t-1} \times \mathrm{Demand}_{c,t-1}) \\ + \beta_2^{(h)}(x_t \times \mathrm{HighDebt}_{j,t-1}) + \beta_3^{(h)}(\mathrm{HighDebt}_{j,t-1} \times \mathrm{Demand}_{c,t-1}) \\ + \delta\, \mathrm{HighDebt}_{j,t-1} + \sum_{p=1}^{4} \phi_p \Delta \log(\mathrm{NTL}_{i,t-p}) + \epsilon_{i,t+h}\end{aligned} \tag{13}$$

We estimate this specification at the land-parcel level incorporating strict city-by-time (week) fixed effects ($\eta_{c,t}$). This demanding specification completely absorbs all unobserved time-varying local macro shocks, such as city-specific policy interventions or aggregate local demand fluctuations.

Figure 8 plots $\beta_1^{(h)}$, the estimated coefficient of the triple interaction term. The results indicate that the coefficient is persistently negative over the 0–20 week horizon, suggesting that the amplification effect of high leverage on construction activity is significantly more pronounced in cities with historically stronger housing demand. In other words, The persistently negative $\beta_1^{(h)}$ resolves this ambiguity in favor of amplification.

In China's real estate sector, pre-sale revenues from off-plan purchases constitute a primary source of internal funding for developers. Highly leveraged firms in high-demand cities are especially dependent on the continuation of strong sales to service debt and finance ongoing construction. When U.S. monetary tightening depresses housing transaction volumes, the absolute decline in pre-sale revenues is mechanically larger in these cities. For financially constrained developers this loss of internal cash flow cannot be offset by additional external debt, forcing sharper declines in construction activity measured by NTL.

To summarize, our evidence suggests that the negative effect of monetary tightening

is amplified in high-demand cities. This result does not contradict our earlier finding that local demand alone does not drive the contraction. Rather, demand conditions operate as an amplifier of the financing mechanism: tighter external financing binds more severely when the internal cash flow buffer is simultaneously weakened by softer local sales. In summary, cleaner identification from the parcel-level evidence suggests that the financing constraint remains the fundamental driver; but local demand powerfully amplifies the financing channel.

4.6 City-level Implications

We conclude by aggregating the firm- and parcel-level evidence to the city level to assess the macroeconomic relevance of the financing channel. In particular, we would like to show that the negative impacts of U.s. monetary tightening on construction activities are bigger for cities with more land purchased by those real estate firms with financial troubles.

To assess the aggregate importance of the financing channel, we relate firm-level exposure to city-level outcomes. We construct a city-level exposure measure based on developer financial conditions (Appendix A). For each city, we define the "bad deal index" as the product of land transaction growth and the aggregated liability ratio. For each city in each year, we identify the listed firm associated with each land transaction. Then, we obtain the financial condition of the corresponding listed firm for each land transaction. In this way, we obtain the associated financial condition for each land transaction. When aggregating the associated financial conditions to the city level, we weight each transaction by either revenue or area of the transaction. A higher "bad deal index" signifies more troubled land transaction in the city. We use the empirical specification in Equation 3. We find that NTL in cities with a higher "bad deal index" declines more after a U.S. tightening, as shown in Figure 9. In other words, cities with greater exposure to financially constrained developers experience significantly larger declines in construction activity following U.S. monetary tightening. This suggests that the financing channel is not only statistically significant but also quantitatively important in explaining cross-sectional variation in the real effects of monetary spillovers.

Consistent with the construction channel, we also find that the contraction is also weaker during winter months in northern cities, when construction activity is largely suspended, providing additional support for the construction-based mechanism (see Appendix C.5).

Taken together, the evidence provides a coherent picture of the transmission mechanism. U.S. monetary tightening worsens firms' external financing conditions, particularly

for those reliant on foreign bond markets. These financing shocks translate into sharp declines in construction activity, especially for highly leveraged firms and in environments where financing constraints are binding. The effects are quantitatively large and account for the bulk of the aggregate response of real activity. These findings establish the construction-financing channel as a central mechanism through which international monetary spillovers operate.

5 External Validity and Cross-Country Evidence

The analysis so far establishes a financing-based transmission mechanism using micro-level data from China. A natural question is whether these patterns extend to other economies. While the identification of the mechanism relies on the unique linkage between parcels, firms, and financing conditions available in the China setting, nighttime light (NTL) data provide a consistent measure of real activity across countries, allowing us to assess the external validity of our findings at a broader level.

We select several of mainland China's neighbors employing weekly NTL, which is similar to our baseline analysis on China.[11] The results are in Figure 10. Two main patterns emerge. First, U.S. monetary tightening has a broadly negative effect on real activity across different economies, consistent with the existence of international spillovers. This finding aligns with the literature documenting global transmission of U.S. monetary policy through financial channels. Second, the contractionary effect is stronger in emerging market economies than in advanced economies. In emerging economies, construction is a key driver of growth and relies heavily on external financing, making it especially sensitive to changes in global financial conditions. The stronger response of NTL in these regions is therefore consistent with a construction-based transmission channel operating through financing costs.

As a supplement, We also extend our results to all economies in the world using monthly NTL data pre-processed by Earth Observation Group (Colorado School of Mines, 2024). The responses are overall negative for most economies and are significantly stronger in countries undergoing rapid urbanization.[12]

Scope and Limitations. A key advantage of NTL data in this context is that measurement is standardized across countries and largely independent of national sta-

[11]The processing of weekly data is very time-consuming, so we only chose several economies for illustration. Emerging market economies include China, Mongolia, Vietnam, Thailand, Bangladesh, and India while advanced economies include Hong Kong (China), Macau (China), Taiwan (China), South Korea, Japan, and Australia.

[12]Results are available upon request.

tistical systems. This mitigates concerns about cross-country comparability that arise when using national accounts data, particularly for emerging economies. While these cross-country results provide suggestive evidence on external validity, they do not allow for direct identification of the underlying mechanism. In particular, the absence of parcel-level and firm-level data prevents us from linking changes in real activity to specific financing conditions or investment decisions. Moreover, the interpretation of NTL differs across levels of development. In emerging markets, NTL is closely tied to construction activity, urban expansion, and industrial production. In advanced economies, it is more strongly associated with service-sector activity and nighttime consumption. As a result, differences in estimated responses may reflect both differences in transmission mechanisms and differences in how NTL maps to real economic activity.

6 Conclusion

This paper studies the international transmission of U.S. monetary policy to real economic activity and identifies a financing-based mechanism through which these effects operate. Using high-frequency monetary policy shocks and nighttime light (NTL) data, we show that U.S. monetary tightening leads to a significant decline in real activity, with the effect concentrated in non-built-up areas associated with construction. By linking parcel-level activity to firm-level financial data, we document that the decline is substantially larger for firms with greater exposure to external financing and for those facing tighter balance sheet constraints. Exploiting the introduction of the "three red lines" policy as a quasi-natural experiment, we further show that tighter financing constraints amplify the sensitivity of construction activity to U.S. monetary shocks. Taken together, these results indicate that U.S. monetary policy affects real activity primarily through external financing costs that operate via construction investment.

A central contribution of the paper is methodological. We show that nighttime light (NTL) data can be used to jointly identify the causal effects and transmission mechanisms of macroeconomic shocks. The high-frequency nature of NTL allows real activity to be aligned with shocks identified in narrow event windows, while its spatial flexibility makes it possible to connect localized activity to underlying economic agents and their characteristics, such as financing conditions. This combination provides a unified empirical framework that moves beyond average effects and directly identifies mechanisms. Because NTL data are available globally and measured consistently across space and time, this approach can be applied broadly to study macroeconomic shocks in other settings, particularly where traditional data are limited.

References

Acosta, M. (2022). The perceived causes of monetary policy surprises. *Published manuscript*.

Bhattarai, S., & Neely, C. J. (2022). An Analysis of the Literature on International Unconventional Monetary Policy. *Journal of Economic Literature*, *60*(2), 527–597. https://doi.org/10.1257/jel.20201493

Bickenbach, F., Bode, E., Nunnenkamp, P., & Söder, M. (2016). Night lights and regional GDP. *Review of World Economics*, *152*(2), 425–447. https://doi.org/10.1007/s10290-016-0246-0

Bluedorn, J. C., & Bowdler, C. (2011). The open economy consequences of U.S. monetary policy. *Journal of International Money and Finance*, *30*(2), 309–336. https://doi.org/10.1016/j.jimonfin.2010.11.001

Bluhm, R., & Krause, M. (2022). Top lights: Bright cities and their contribution to economic development. *Journal of Development Economics*, *157*, 102880. https://doi.org/10.1016/j.jdeveco.2022.102880

Bräuning, F., & Ivashina, V. (2020). U.s. monetary policy and emerging market credit cycles. *Journal of Monetary Economics*, *112*, 57–76.

Chor, D., & Li, B. (2024). Illuminating the effects of the US-China tariff war on China's economy. *Journal of International Economics*, *150*, 103926. https://doi.org/10.1016/j.jinteco.2024.103926

Colorado School of Mines. (2024). Earth Observation Group - Payne Institute for Public Policy. https://payneinstitute.mines.edu/eog/

Dedola, L., Rivolta, G., & Stracca, L. (2017). If the Fed sneezes, who catches a cold? *Journal of International Economics*, *108*, S23–S41. https://doi.org/10.1016/j.jinteco.2017.01.002

Elvidge, C. D., Zhizhin, M., Ghosh, T., Hsu, F.-C., & Taneja, J. (2021). Annual Time Series of Global VIIRS Nighttime Lights Derived from Monthly Averages: 2012 to 2019. *Remote Sensing*, *13*(5), 922. https://doi.org/10.3390/rs13050922

Georgiadis, G. (2016). Determinants of global spillovers from US monetary policy. *Journal of International Money and Finance*, *67*, 41–61. https://doi.org/10.1016/j.jimonfin.2015.06.010

Gibson, J., Olivia, S., Boe-Gibson, G., & Li, C. (2021). Which night lights data should we use in economics, and where? *Journal of Development Economics*, *149*, 102602. https://doi.org/10.1016/j.jdeveco.2020.102602

Gibson, J., Zhang, X., Park, A., Yi, J., & Xi, L. (2024). *Remotely measuring rural economic activity and poverty: Do we just need better sensors?* (CEI Working Paper Series No. 2023-08). Center for Economic Institutions, Institute of Economic Research, Hitotsubashi University. https://ideas.repec.org/p/hit/hitcei/2023-08.html

Gopinath, G., Boz, E., Casas, C., Díez, F. J., Gourinchas, P.-O., & Plagborg-Møller, M. (2020). Dominant Currency Paradigm. *American Economic Review*, *110*(3), 677–719. https://doi.org/10.1257/aer.20171201

Gürkaynak, R., Karasoy-Can, H. G., & Lee, S. S. (2022). Stock Market's Assessment of Monetary Policy Transmission: The Cash Flow Effect. *The Journal of Finance*, *77*(4), 2375–2421. https://doi.org/10.1111/jofi.13163

Gürkaynak, R., & Sack, B. (2005, November). *Do Actions Speak Louder Than Words? The Response of Asset Prices to Monetary Policy Actions and Statements* (Computing in Economics and Finance 2005 No. 323). Society for Computational Economics.

Retrieved August 9, 2024, from https://econpapers.repec.org/paper/scescecf5/323.htm

Gürkaynaka, R., Sack, B., & Swanson, E. (2005). Do Actions Speak Louder Than Words? The Response of Asset Prices to Monetary Policy Actions and Statements. *International Journal of Central Banking*, *1*(1), 55–93. https://www.ijcb.org/journal/v1n1/do-actions-speak-louder-words-response-asset-prices-monetary-policy-actions-and

Henderson, J. V., Storeygard, A., & Weil, D. N. (2012). Measuring Economic Growth from Outer Space. *American Economic Review*, *102*(2), 994–1028. https://doi.org/10.1257/aer.102.2.994

Huang, Y., Panizza, U., & Portes, R. (2024). Corporate foreign bond issuance and interfirm loans in China. *Journal of International Economics*, *152*, 103975. https://doi.org/10.1016/j.jinteco.2024.103975

Jarociński, M. (2024). Estimating the Fed's unconventional policy shocks. *Journal of Monetary Economics*, *144*, 103548. https://doi.org/10.1016/j.jmoneco.2024.01.001

Jiang, H., Sun, Z., Guo, H., Xing, Q., Du, W., & Cai, G. (2022). A standardized dataset of built-up areas of China's cities with populations over 300,000 for the period 1990–2015. *Big Earth Data*, *6*(1), 103–126. https://doi.org/10.1080/20964471.2021.1950351

Jordà, Ò. (2005). Estimation and Inference of Impulse Responses by Local Projections. *American Economic Review*, *95*(1), 161–182. https://doi.org/10.1257/0002828053828518

Kim, J., Kim, K., Park, S., & Sun, C. (2022). The Economic Costs of Trade Sanctions: Evidence from North Korea. *SSRN Electronic Journal*. https://doi.org/10.2139/ssrn.4032573

Kim, S. (2001). International transmission of U.S. monetary policy shocks: Evidence from VAR's. *Journal of Monetary Economics*, *48*(2), 339–372. https://doi.org/10.1016/S0304-3932(01)00080-0

Kubota, H., & Shintani, M. (2022). High-frequency identification of monetary policy shocks in Japan. *The Japanese Economic Review*, *73*(3), 483–513. https://doi.org/10.1007/s42973-021-00110-x

Lakdawala, A., Moreland, T., & Schaffer, M. (2021). The international spillover effects of US monetary policy uncertainty. *Journal of International Economics*, *133*, 103525. https://doi.org/10.1016/j.jinteco.2021.103525

Maćkowiak, B. (2007). External shocks, U.S. monetary policy and macroeconomic fluctuations in emerging markets. *Journal of Monetary Economics*, *54*(8), 2512–2520. https://doi.org/10.1016/j.jmoneco.2007.06.021

Martínez, L. R. (2022). How Much Should We Trust the Dictator's GDP Growth Estimates? *Journal of Political Economy*, *130*(10), 2731–2769. https://doi.org/10.1086/720458

Michalopoulos, S., & Papaioannou, E. (2018). Spatial Patterns of Development: A Meso Approach. *Annual Review of Economics*, *10*(1), 383–410. https://doi.org/10.1146/annurev-economics-080217-053355

Miranda-Agrippino, S., & Nenova, T. (2022). A tale of two global monetary policies. *Journal of International Economics*, *136*, 103606. https://doi.org/10.1016/j.jinteco.2022.103606

Miranda-Agrippino, S., & Rey, H. (2020). U.S. Monetary Policy and the Global Financial Cycle. *The Review of Economic Studies*, *87*(6), 2754–2776. https://doi.org/10.1093/restud/rdaa019

Miranda-Agrippino, S., & Ricco, G. (2021). The Transmission of Monetary Policy Shocks. *American Economic Journal: Macroeconomics*, *13*(3), 74–107. https://doi.org/10.1257/mac.20180124

Nakamura, E., & Steinsson, J. (2018). High-Frequency Identification of Monetary Non-Neutrality: The Information Effect*. *The Quarterly Journal of Economics*, *133*(3), 1283–1330. https://doi.org/10.1093/qje/qjy004

Pinkovskiy, M., & Sala-i-Martin, X. (2016). Lights, Camera … Income! Illuminating the National Accounts-Household Surveys Debate. *Quarterly Journal of Economics*, *131*(2), 579–631. https://doi.org/10.1093/qje/qjw003

Rogers, J. H., Sun, B., & Sun, T. (2024). U.S.-China Tension. *SSRN Electronic Journal*. https://doi.org/10.2139/ssrn.4815838

Rossi-Hansberg, E., & Zhang, J. (2025, February). *Local GDP Estimates Around the World* (tech. rep. No. w33458). National Bureau of Economic Research. Cambridge, MA. https://doi.org/10.3386/w33458

Rudebusch, G. D. (1998). Do Measures of Monetary Policy in a Var Make Sense? *International Economic Review*, *39*(4), 907. https://doi.org/10.2307/2527344

Shieh, H. (2024). Can you hear me now? Identifying the effect of Chinese monetary policy announcements. *Journal of International Money and Finance*, *144*, 103078. https://doi.org/10.1016/j.jimonfin.2024.103078

Swanson, E. T. (2021). Measuring the effects of federal reserve forward guidance and asset purchases on financial markets. *Journal of Monetary Economics*, *118*, 32–53. https://doi.org/10.1016/j.jmoneco.2020.09.003

Uribe, M., & Yue, V. Z. (2006). Country spreads and emerging countries: Who drives whom? *Journal of International Economics*, *69*(1), 6–36. https://doi.org/10.1016/j.jinteco.2005.04.003

Tables

Table 1: Real Estate Firm Foreign and Domestic Bond Issue Net Standing Value (Scaled by Operation Indicator) Responses to MPs

Panel A: Foreign Bond

	/ Asset	/ Liability	/ Current Liability	/ Long-term Liability
MPs	-0.0598***	-0.0801***	-0.1298***	-0.6261+
	(0.0140)	(0.0199)	(0.0362)	(0.3868)
Firm FE	Yes	Yes	Yes	Yes
N	2,238	2,238	2,238	2,226
R^2	0.3390	0.3371	0.3616	0.1860

Panel B: Domestic Bond

	/ Asset	/ Liability	/ Current Liability	/ Long-term Liability
MPs	-0.0143	0.0891	0.0238	-1.9571
	(0.0819)	(0.2804)	(0.2952)	(1.6913)
Firm FE	Yes	Yes	Yes	Yes
N	3,955	3,955	3,955	3,862
R^2	0.4900	0.5744	0.5388	0.2400

Notes: Significance levels are based on Clustered (Firm) standard-errors. Significance Codes: ***: 0.01, **: 0.05, *: 0.1, +: 0.2.

Table 2: Real Estate Firm Interest Expense (Scaled by Operation Indicator) Responses to MPs

	Interest Expense / Asset	Interest Expense / Liability	Interest Expense / Current Liability
MPs	3.1900***	3.7483***	2.9784***
	(0.7028)	(0.7870)	(0.7943)
Firm FE	Yes	Yes	Yes
N	4,832	4,832	4,831
R^2	0.8216	0.8175	0.8130

Notes: Significance levels are based on Clustered (Firm) standard-errors. Significance Codes: ***: 0.01, **: 0.05, *: 0.1, +: 0.2.

Figures

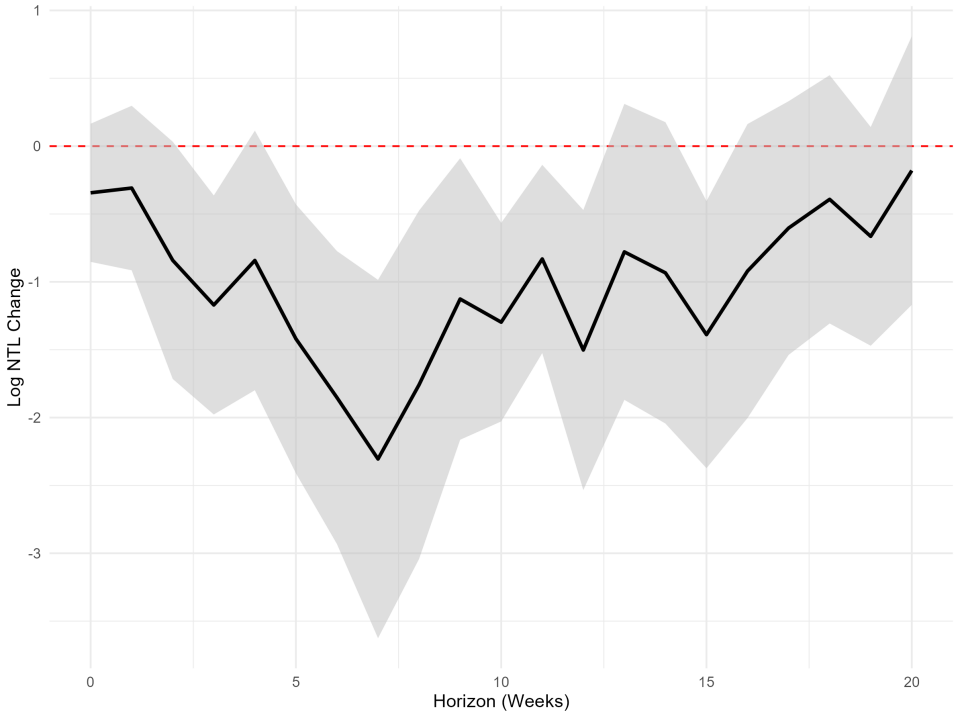

Figure 1: Response of NTL to U.S. MPs: National Aggregate, Baseline

Notes: The solid line plots the estimated impulse response ($\beta^{(h)}$) of the cumulative change in aggregate log nighttime lights to a contractionary U.S. monetary policy shock (MPS), estimated via the local projection specification: $y_{t+h} - y_{t-1} = \alpha^{(h)} + \sum_{q=1}^{Q} \phi_q^{(h)} \Delta y_{t-q} + \beta^{(h)} x_t + u_{t+h|t}$. The horizontal axis denotes the response horizon in weeks ($h = 0$ to 20). The U.S. MPS (x_t) is aggregated to the weekly frequency consistent with the dependent variable. The model controls for four lags of the differenced dependent variable ($Q = 4$), selected by the Akaike Information Criterion (AIC), results remain robust under the BIC criterion. The sample period is from 2012 to 2023. The shaded bands represent the 90 percent confidence intervals, constructed using Newey-West standard errors.

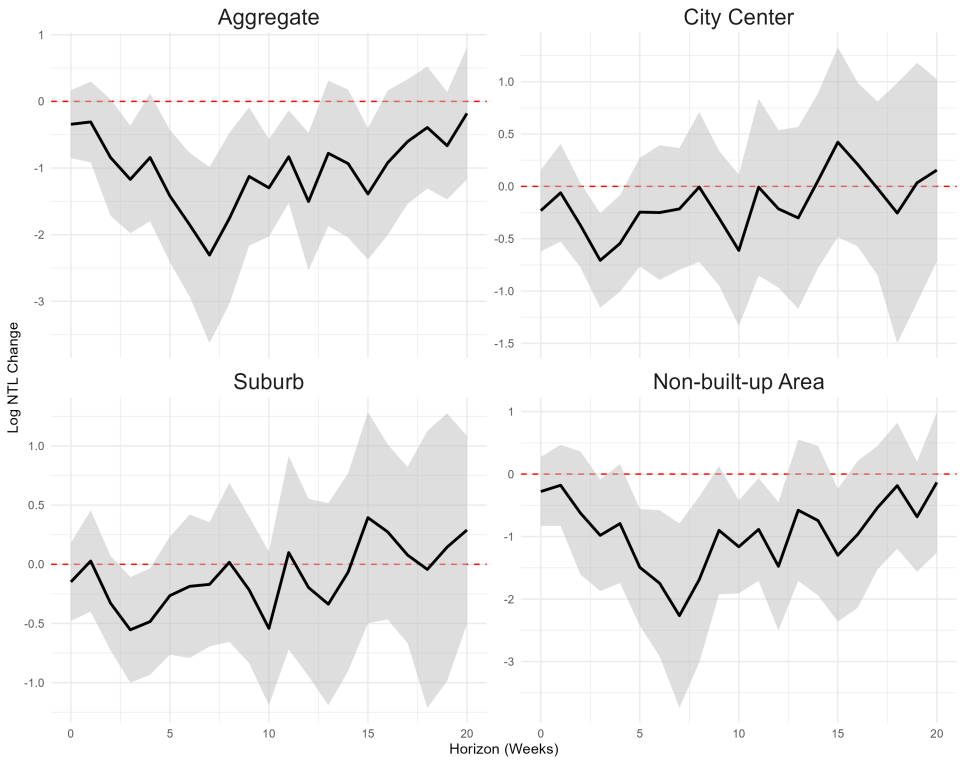

Figure 2: Response of NTL to U.S. MPs: City Areas Decomposition

Notes: This graph plots the estimated impulse responses of the cumulative change in aggregate log nighttime lights across different city areas (City Center, Suburb, and Non-built-up Area) to a contractionary U.S. monetary policy shock. The areas are characterized by service, manufacturing, and construction activities, respectively. The specification is identical to the baseline local projection: $y_{t+h} - y_{t-1} = \alpha^{(h)} + \sum_{q=1}^{4} \phi_q^{(h)} \Delta y_{t-q} + \beta_0^{(h)} x_t + u_{t+h|t}$. The horizontal axis denotes the response horizon in weeks ($h = 0$ to 20). The sample period is from 2012 to 2023. The shaded bands represent the 90 percent confidence intervals, constructed using Newey-West standard errors.

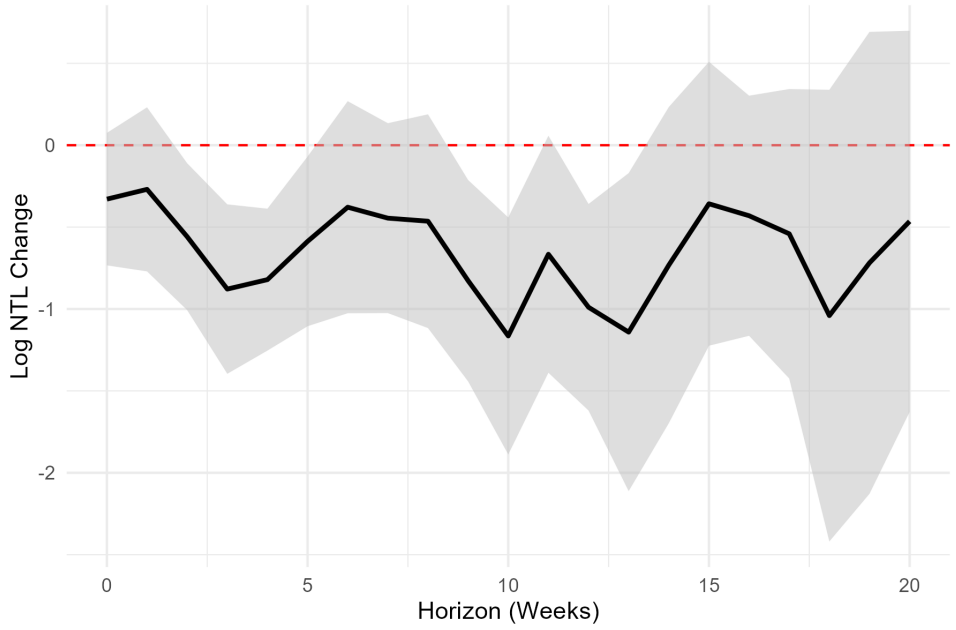

Figure 3: Response of NTL to U.S. MPs: Transacted Lands by Real Estate Firms

Notes: This graph plots the estimated impulse response of the cumulative change in aggregate log nighttime lights (NTL) in transacted lands to a contractionary U.S. monetary policy shock (MPS). The aggregate time-series response is calculated across all lands purchased by listed real estate firms. The specification is identical to the baseline. The sample spans from 2012 to 2023. The U.S. MPS is aggregated to the weekly frequency consistent with the dependent variable. The shaded bands represent the 90 percent confidence intervals, constructed using Newey-West standard errors.

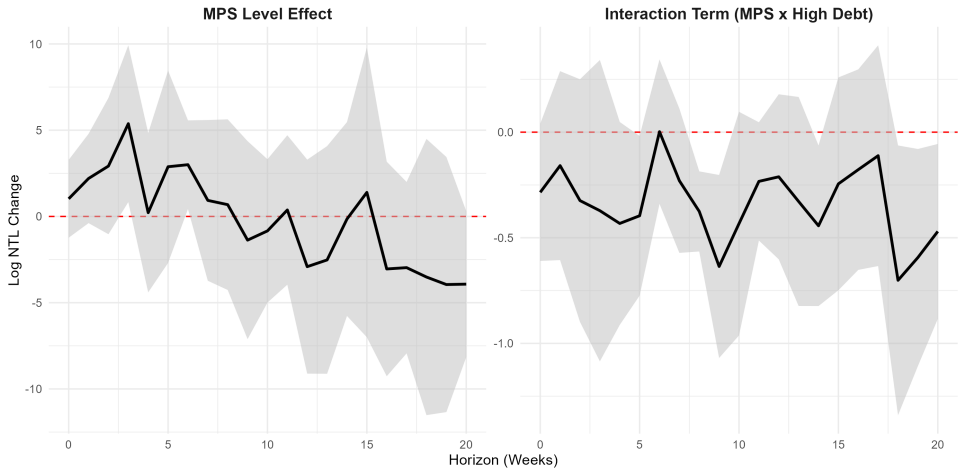

Figure 4: Response of NTL to U.S. MPs: The Role of Firm Debt

Notes: This graph plots the estimated impulse responses of the cumulative change in aggregate log nighttime lights (NTL) at the firm level to a contractionary U.S. monetary policy shock (MPS). The left panel shows the main effect of the U.S. MPS ($\beta_1^{(h)}$), while the right panel shows the differential response ($\beta_2^{(h)}$) for highly leveraged firms, estimated via the local projection specification: $y_{i,t+h} - y_{i,t-1} = \alpha_i^{(h)} + \sum_{q=1}^{4} \phi_q^{(h)} \Delta y_{i,t-q} + \beta_1^{(h)} x_t + \beta_2^{(h)} x_t s_{i,t-L} + \beta_3^{(h)} s_{i,t-L} + \gamma^{(h)} W_{i,t-L} + u_{i,t+h|t}$. Here, $s_{i,t-L}$ is a dummy indicating whether the firm's debt-to-asset ratio is above the sample median in the previous quarter. The specification controls for firm fixed effects ($\alpha_i^{(h)}$), firm-level controls ($W_{i,t-L}$: lagged log assets and profit-to-revenue ratio) along with their interactions with the U.S. MPS (x_t), and four lags of the dependent variable. The U.S. MPS is aggregated to the weekly frequency. The shaded bands represent the 90 percent confidence intervals, constructed using two-way clustered standard errors at the firm and week levels.

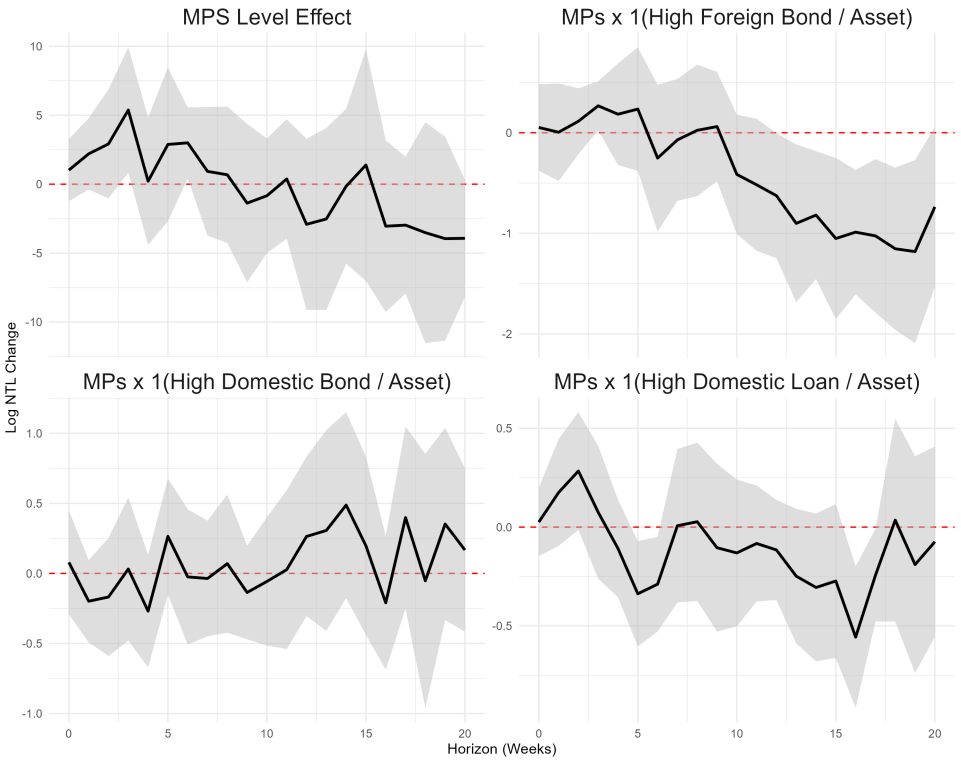

Figure 5: Response of NTL to U.S. MPs: Firm Debt Components

Notes: This graph plots the estimated impulse responses of the cumulative change in aggregate log nighttime lights (NTL) at the firm level to a contractionary U.S. monetary policy shock (MPS) across different debt components. The local projection is specified as: $y_{i,t+h} - y_{i,t-1} = \alpha_i^{(h)} + \sum_{q=1}^{4} \phi_q^{(h)} \Delta y_{i,t-q} + \beta_1^{(h)} x_t + \beta_{FB}^{(h)} x_t s_{i,t-L}^{FB} + \beta_{DB}^{(h)} x_t s_{i,t-L}^{DB} + \beta_{DL}^{(h)} x_t s_{i,t-L}^{DL} + \cdots + \gamma^{(h)} W_{i,t-L} + u_{i,t+h|t}$. The dummy variables $s_{i,t-L}^{FB}$, $s_{i,t-L}^{DB}$, and $s_{i,t-L}^{DL}$ equal 1 if the firm's ratio of foreign bonds, domestic bonds, and domestic loans to total assets is above the sample median in the previous quarter, respectively. The panels display the main effect ($\beta_1^{(h)}$) and the differential responses for foreign bonds ($\beta_{FB}^{(h)}$), domestic bonds ($\beta_{DB}^{(h)}$), and domestic loans ($\beta_{DL}^{(h)}$). The U.S. MPS (x_t) is aggregated to the weekly frequency. The shaded bands represent the 90 percent confidence intervals, constructed using two-way clustered standard errors at the firm and week levels.

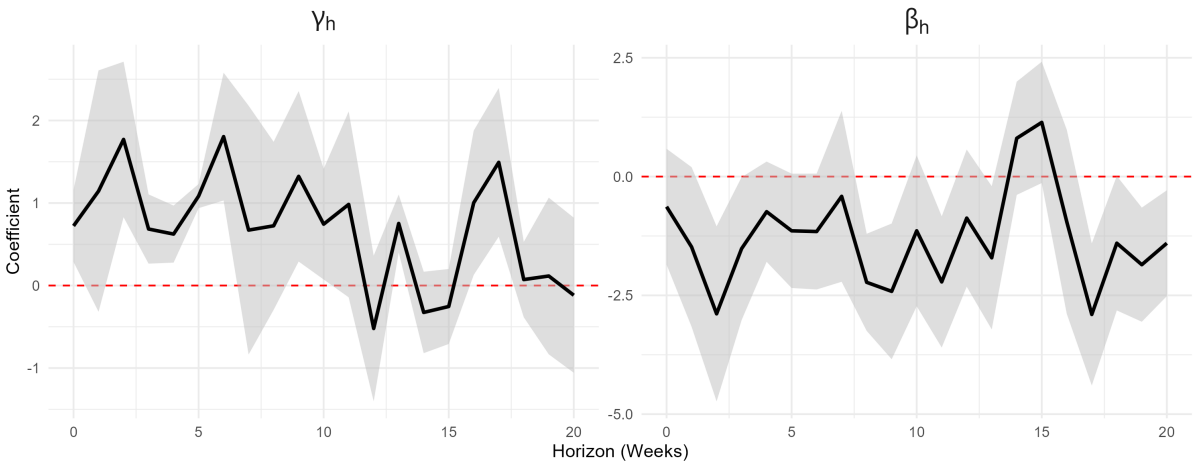

Figure 6: Response of NTL to U.S. MPs: Three Red Line Policy

Notes: This graph plots the estimated impulse responses of the cumulative change in aggregate log nighttime lights (NTL) in transacted lands to a contractionary U.S. monetary policy shock (MPS) around the implementation of the "Three Red Lines" policy. The sample covers a 2-year window (2020–2021) centered on the policy implementation date (August 20, 2020). The local projection is specified as: $y_{i,t+h} - y_{i,t-1} = \alpha_i^{(h)} + \alpha_t^{(h)} + \sum_{q=1}^{4} \phi_q^{(h)} \Delta y_{i,t-q} + \beta_j^{(h)} x_t \cdot Policy_t \cdot Cross_i^j + \gamma_j^{(h)} x_t \cdot Cross_i^j + \delta_j^{(h)} Policy_t \cdot Cross_i^j + \theta_j^{(h)} W_{i,t-L} + u_{i,t+h|t}$. Here, $Policy_t$ is a dummy equal to 1 after the policy implementation, and $Cross_i^j$ is a time-invariant dummy indicating whether the firm breached the short-term debt red line (cash-to-short-term debt ratio < 1) in 2019. The left panel shows the pre-policy differential response ($\gamma^{(h)}$), and the right panel shows the additional differential response after the policy ($\beta^{(h)}$). The specification controls for firm and time fixed effects ($\alpha_i^{(h)}$, $\alpha_t^{(h)}$), and firm-level controls ($W_{i,t-L}$). The U.S. MPS (x_t) is aggregated to the weekly frequency. The shaded bands represent the 90 percent confidence intervals, constructed using two-way clustered standard errors at the firm and week levels.

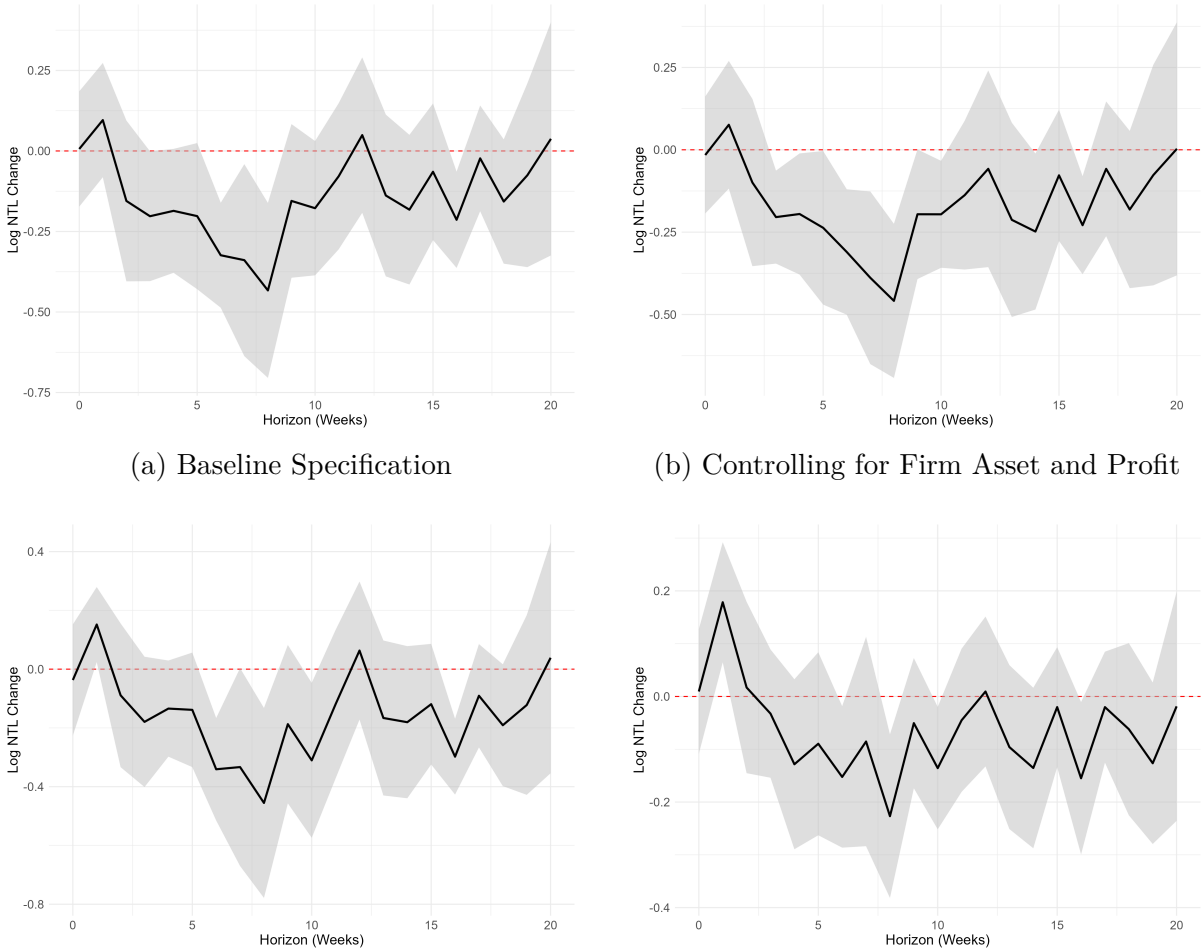

(a) Baseline Specification

(b) Controlling for Firm Asset and Profit

(c) Controlling for Local Housing Demand

(d) City × Time Fixed Effects

Figure 7: Response of NTL to U.S. MPs: The Role of Firm Debt, Land Parcel Level

Notes: This graph plots the estimated impulse response functions (IRFs) using the local projections framework (Jordà, 2005) at the weekly frequency. Panel (a) estimates the baseline specification: $\Delta_h \log(NTL_{i,t+h}) = \alpha_i + \gamma_t + \beta^{(h)}(MPS_t \times HighDebt_{j,t-1}) + \delta HighDebt_{j,t-1} + \sum_{p=1}^{4} \phi_p \Delta \log(NTL_{i,t-p}) + \epsilon_{i,t+h}$. Panel (b) additionally controls for the firm's lagged log asset and profit ratio, along with their interactions with MPS_t. Panel (c) includes concurrent local housing demand (floor space sold per capita). Results are robust if instead controlling lagged demand and its interaction with monetary surprise. Panel (d) employs stringent City × Time fixed effects. In all panels, the solid black line reports the estimated coefficients on the primary interaction term ($MPS_t \times HighDebt_{j,t-1}$). The sample excludes the broad COVID-19 period from 2020-2022. Shaded areas represent 90% confidence intervals based on two-way clustered standard errors at the parcel and week levels.

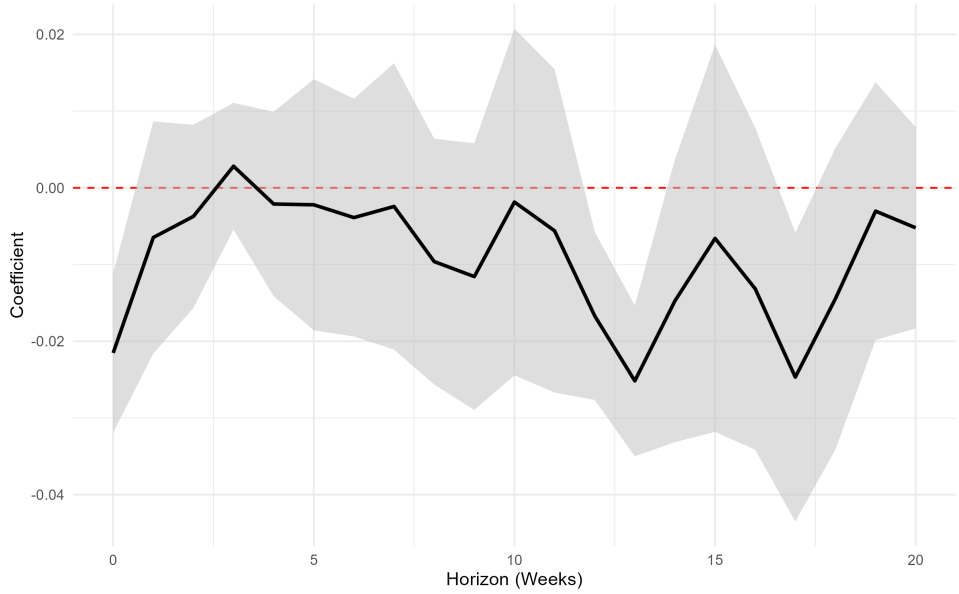

Figure 8: Response of NTL to U.S. MPs: Interaction of Debt Ratio and Housing Demand

Notes: This graph plots the estimated coefficient of the triple interaction term ($\beta_1^{(h)}$) between the U.S. monetary policy shock (x_t), the firm's high-debt dummy ($HighDebt_{j,t-1}$), and the city's housing demand ($Demand_{c,t-1}$), estimated at the land-parcel level. The local projection is specified as: $\Delta_h \log(\text{NTL}_{i,t+h}) = \alpha_i + \eta_{c,t} + \beta_1^{(h)}(x_t \times \text{HighDebt}_{j,t-1} \times \text{Demand}_{c,t-1}) + \cdots + \sum_{p=1}^{4} \phi_p \Delta \log(\text{NTL}_{i,t-p}) + \epsilon_{i,t+h}$. The specification strictly controls for parcel fixed effects (α_i) and city-by-week fixed effects ($\eta_{c,t}$) to absorb unobserved local macro shocks. The shaded bands represent the 90 percent confidence intervals generated based on standard errors clustered at the land parcel and week levels.

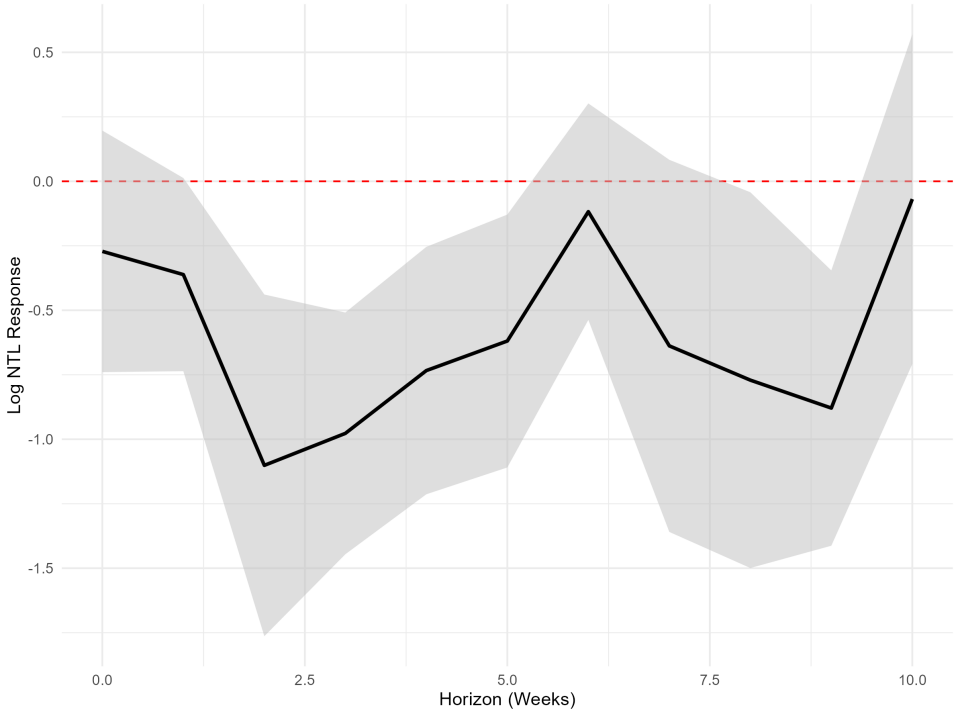

Figure 9: NTL Response to Interaction of U.S. MPs: Bad Deal Index

Notes: This graph plots the differential response of city-level nighttime lights (NTL) to U.S. monetary policy shocks based on the city's exposure to financially constrained developers. The city-level exposure measure ("bad deal index") is defined as the product of land transaction growth and the aggregated liability ratio of developers who purchased land in that city, weighted by transaction revenue. The shaded bands represent the 90 percent confidence intervals generated based on standard errors clustered at the city and week levels.

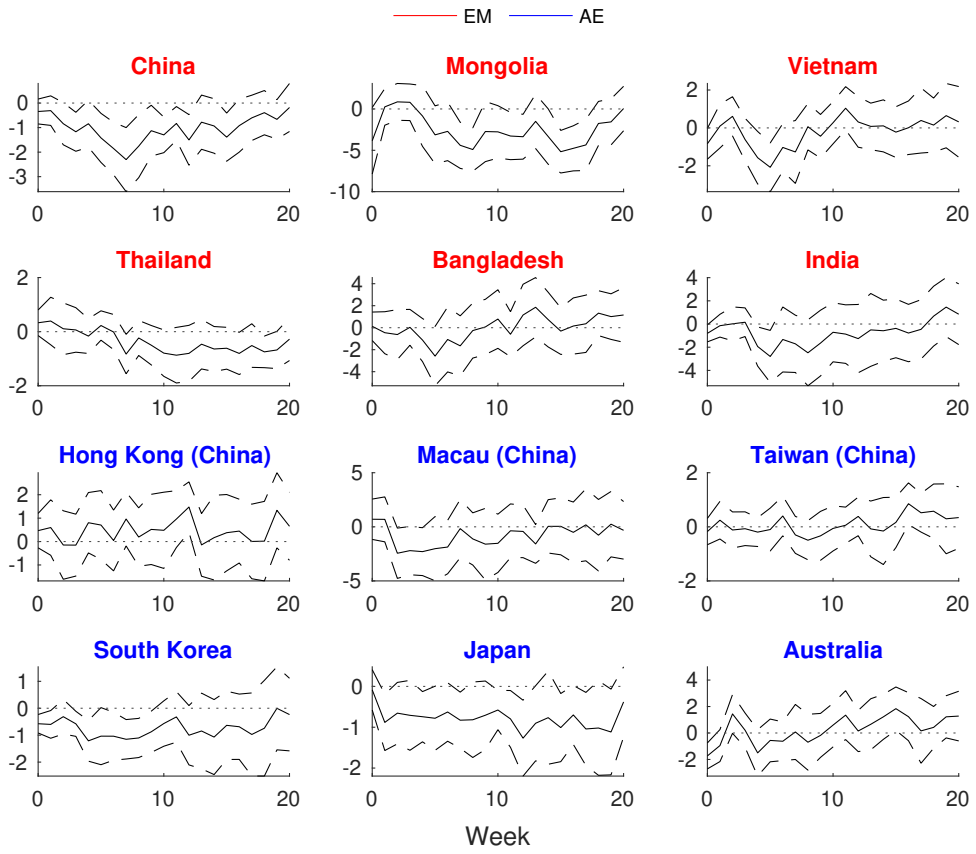

Figure 10: Response of NTL to U.S. MPs: Across Economies

Notes: This graph plots the estimated impulse responses of aggregate nighttime lights (NTL) to U.S. monetary policy shocks across different economies (emerging markets vs. advanced economies). We apply the baseline local projection specification on different economies respectively. The U.S. MPS is aggregated to the weekly frequency consistent with the dependent variable. The dashed ribbons are the 90 percent confidence intervals generated based on the Newey-West standard errors.

Appendix A Data Appendix

This appendix provides details on data construction, variable definitions, and validation exercises. The empirical design combines three components: (i) high-frequency U.S. monetary policy shocks, (ii) nighttime light (NTL) data as a proxy for real activity, and (iii) micro-level data linking land transactions to firm-level financial information. We describe each component in turn and document the procedures used to construct the integrated dataset.

A.1 Monetary policy shock

Our baseline monetary policy shock is constructed using high-frequency changes in federal funds futures prices around FOMC announcements, following Gürkaynak et al. (2005). The data are obtained from Jarociński (2024).

For robustness, we also consider alternative measures, including the monetary policy shock series constructed by Acosta (2022) and decompositions distinguishing conventional and unconventional components.

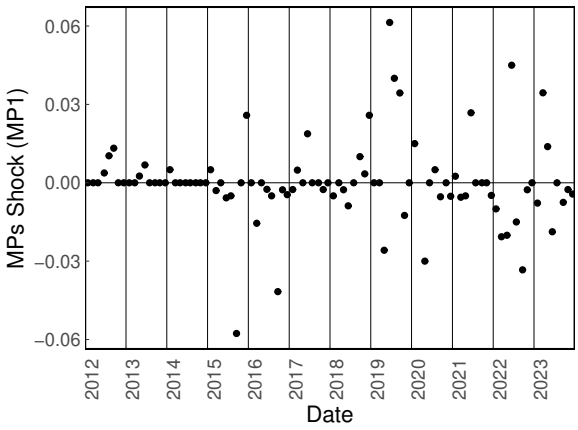

Figure A.1: Proxies of Monetary Policy Shock: Baseline

Notes: For each MPs event, the corresponding date is the day when the FOMC is held.

Table A.1: Summary Statistics: Monetary Policy Shock

	N	Mean	SD	Min	Max
Year	99	2017.61	3.49	2012.00	2024.00
Month	99	6.62	3.56	1.00	12.00
Day	99	17.95	9.36	1.00	31.00
MPs: MP1	95	0.0001	0.02	-0.06	0.06

Notes: The last day with non-zero baseline MPs: MP1 is on 2023-12-13. Only dates with MPs are included.

A.2 Details of NTL Data

We use nighttime light (NTL) data from NASA's Black Marble product (VIIRS), available at daily frequency from 2012 onward. The data provide global coverage with consistent measurement across space and time.

For the global analysis, we combine VIIRS data (post-2014) with DMSP data (pre-2014). We harmonize the two series using a conversion factor estimated from overlapping years, ensuring consistency in levels and trends.

Frequency aggregation. We aggregate daily NTL to the weekly frequency to align with the timing of monetary policy shocks and reduce high-frequency noise.

Daily NTL The raw daily data are available on the official website of NASA at: https://ladsweb.modaps.eosdis.nasa.gov/missions-and-measurements/products/VNP46A2, and Google Earth Engine (GEE) at: https://developers.google.com/earth-engine/datasets/catalog/NOAA_VIIRS_001_VNP46A2. In this paper, the daily NTL data is derived from NASA's Black Marble product using the VIIRS instrument (NASA 2020). The product code of the stray light-corrected daily NTL series is VNP46A2. It corrects for stray light, such as wildfire and moonlight. It also adjusts for the satellite angle that varies each day when the satellite captures the image of the same place.

As an illustration, the map of NTL in the East Asia and Pacific region released by NASA in 2016 is as follows.[13]

Figure A.2: Nighttime Luminosity Captured by NASA Satellite in 2016

Monthly and Annual NTL The monthly NTL series has been available since April 2012. We use the stray-light corrected monthly series when studying the country-level

[13]The original file is publicly available at:
https://www.nasa.gov/specials/blackmarble/media/BlackMarble20161km.jpg.

NTL response to U.S. MPs, as it is available globally without the necessity for post-processing.[14] The annual series has been available since 2012 (Elvidge et al., 2021).[15] This data is used to investigate the correlation between NTL and GDP across countries. The processed monthly and annual datasets are publicly available on the Earth Observation Group (EOG) website hosted by the Colorado School of Mines at: https://payneinstitute.mines.edu/eog/. EOG processes original satellite images to filter out ephemeral lights such as fire.

NTL is widely used as a proxy for economic activity and is strongly correlated with GDP, particularly in developing economies. We provide additional validation in Appendix D.

A.2.1 Daily NTL Data Processing

The NTL data are from NASA's Black Marble with public access dating back to 19 January 2012. We use the period until the end of 2023. The original data are in daily frequency, which is convenient for event studies to obtain a sharper identification of the policy impacts around FOMC announcements.

The NTL data are quite granular, where a pixel in the digitalized image corresponds to 15 arc seconds out of 360 degrees in both latitude and longitude, converting to 464m on the equator. These cells are small enough to identify economic activities at almost any regional level (e.g. a sub-city area or even a land of a real estate firm), which greatly facilitates the identification of the causal impacts and the associated transmission mechanism.[16]

The data are captured by satellites with the VIIRS (Visible Infrared Imaging Radiometer Suite) instrument, which is the latest and the most accurate version of Suomi Polar-orbiting Partnership jointly by NASA and NOAA.[17] Unlike the previous generation of satellite images for NTL, the DMSP, the VIIRS is time consistent (Gibson et al., 2021; Rossi-Hansberg & Zhang, 2025), which supports the intertemporal comparison required in the study. It also has no top-coding problems (Bluhm & Krause, 2022), a vital issue when measuring in bright places, such as the city center. The neighboring cells are not autocorrelated (Michalopoulos & Papaioannou, 2018), which enables precisely distinguishing light sources at the cell level. We use the Black Marble VIIRS product VNP46A2, which applies the Bidirectional Reflectance Distribution Function (BRDF) on the raw satellite image. It removes distraction factors such as stray light and moonlight. It also adjusts the satellite angle, which varies daily when the satellite captures the image

[14] The monthly series without stray-light correction is unavailable in summer in places with higher latitudes due to long daytime and even longer astronomical light in summer.

[15] The annual NTL data in 2012 is derived from April to December, while the annual data in forwarding years are all derived from corresponding monthly series from January to December in the same year. Before 2014, the summation is over the monthly series without stray-light correction. Since 2014, the derivation is based on the stray light-corrected monthly series.

[16] Once the NTL of a construction field is identified, it can be matched with the associated real estate firm using land transaction records. The granular nature of these NTL data also allows the matching of NTL to each subarea within a city, namely the city center, the suburb and the nonbuilt-up area according to the spatial boundaries.

[17] For details of the data sources, see Appendix A.2. A web-based interface of the VIIRS light map is available at: https://www.lightpollutionmap.info (light pollution map).

at the same place. Additionally, the product labels cells contaminated by cloud and snow covers, enabling our further processing to remove such noises.

We use cloud computers to process the big data at the cell level. To conduct city-level analysis, we also generate aggregated daily NTL series for 345 out of 367 cities (prefectures) in mainland China. For each of the 4,332 available days, there are 55,404,633 cells for the whole country.[18][19] The detailed process is in Appendix A.2.1.

We match the NTL with MPs data after aggregating them to weekly frequency.[20] This substantially reduces the noise while keeping the frequency sufficiently high to identify the MPs impact on the real economy. Meanwhile, as FOMC is conducted every six weeks on average, converting the daily series to weekly does not have overlapping issues. We assign each MPs value to the week of the FOMC date and interpolate the weeks with no FOMC meetings as having zero shocks.

We illustrate that NTL significantly and positively correlates with traditional economic activity indicators, such as GDP. Figure B.1 shows such associations at annual frequency and the city level. We also display this correlation across periods/industries/countries. See Appendix B for more details.

Raw Data Processing To smooth the cloud computing process on the Google Cloud Platform (GCP), we use the Google Earth Engine (GEE) repository to capture the daily NTL geospatial data. Firstly, we extract the map using a rectangle with longitudes from 75 to 135 degrees and latitudes from 18 to 53 degrees. The rectangle contains the whole land area of mainland China.[21] For each day's NTL data, we save four layers to the corresponding TIFF file: daily NTL (DNB_BRDF_Corrected_NTL), NASA-filled daily NTL (Gap_Filled_DNB_BRDF_ Corrected_NTL), quality flag (Mandatory_Quality_Flag), and snow flag (Snow_Flag). We do this for each day from 19 January 2012 to 31 December 2023 with 2,174 files.

NTL Series Construction (1) *Cell Series*: We filter out cells with contaminated daily NTL (e.g. by cloud or snow) and fill them with previous values. For each cell (defined by longitude and latitude), we keep the daily NTL value only if both the quality flag and the snow flag are zero, indicating no quality (e.g., cloud coverage) issue or snow-coverage issue in the cell. Then, we concatenate the dataset to a cell-level daily panel. For each cell, we obtain a time series with several missing values for the daily NTL. We fill the NA values with the latest valid value from the beginning to the end. Then, we fill the starting NA values using the earliest valid value, so the time series of each cell is fully

[18]The remaining 22 cities are large in area but have relatively small populations and economic activities. The processing time on cloud computers positively correlates with the area processed. Therefore, we drop them off in the processing for budget and time considerations.

[19]When aggregating the geospatial data at the city level, the shape files of the administrative boundaries of the cities we use are derived from the official source (National Bureau of Statistics of China, henceforth NBSC) with revisions to show the updated boundaries across cities in 2022.

[20]Every week is defined as from a Sunday to the closest upcoming Saturday (included).

[21]For Hainan province, we use another rectangle with longitudes from 108 to 112 degrees and latitudes from 17 to 21 degrees. We omit Sansha, a remote city with a small area far from the main body of Hainan Island.

filled. We call the filled daily NTL series the manually-filled NTL series. For each of the 4,332 available days, there are 55,404,633 cells for the whole country.

(2) *City Series*: Then, we concatenate the time series for each city, and the merged dataset is a city-level daily panel. The key variables in the panel include the city code and the date. For each city, we use the GIS (Geographic Information System) shape file.[22] We crop from the daily rectangles using the shape file. For the cropped dataset, we filter out observations without NASA-filled daily NTL (very few cases), as the value is supposed to be available for every legible cell on the map. The cropped dataset includes longitude, latitude, and the values of the four layers for each cell. For computational efficiency, we exclude cities with more than 500,000 cells. Consequently, we generate aggregated daily NTL series for 345 out of 367 cities (prefectures) in mainland China. For each city on each day, we record the number of valid cells and the sum of NTL. In the aggregated daily NTL series, we drop the dates where the valid cell numbers are less than 90 percent of the maximum cell number for either the NASA-filled NTL or the manually-filled NTL. Using the sum of NTL divided by the number of cells, we obtain the average NTL for each city on each day. The summary statistics of NTL in the weekly/city level are show in Table A.2.

Table A.2: Summary Statistics: Weekly NTL, City

	N	Mean	SD	Min	Max
Year	214793	2017.51	3.45	2012.00	2023.00
Month	214793	6.54	3.45	1.00	12.00
Day	214793	15.70	8.79	1.00	31.00
Sum of NTL	214793	86803.02	88277.75	382.97	1943628.94
Number of cell	214793	85543.86	85234.57	427.00	491798.00

Notes: The unit of NTL in each cell is average radiation (nW/cm2/sr). For each city, NTL are aggregated to week level by average. A week starts from Sunday.

(3) *National Series*: Finally, we also aggregate the city-level panel into a national-level daily NTL time series. For each day, we calculate the national average NTL weighted by the number of cells of each city.

Built-up Area We also apply the GIS shape file for the built-up area to crop from the daily rectangles. Similar to the city-level daily panel of NTL, we generate a city-level daily panel of NTL for each definition of built-up area: city center, suburb, and non-built-up area. The variables in the panel include the date, city code, city area, NTL, and the definition year of the built-up area (each five years from 1990 to 2015). Similarly, for each city area, we also aggregate it to a national weighted level time series.

[22]The shape files used to crop the GeoTiff files of NTL are from NewHorizon, a third-party provider of China's GIS information, most recently updated in 2022. They are based on the official shape files published by the National Bureau of Statistics of China (NBSC) with minor corrections to reflect the latest administrative division. Using the official shape files published by the NBSC in 2020 does not substantially change the results of the study.

Mountain Areas To remove mountain areas and other unhabitable areas in China, we use the land cover map from CLCD.[23] The geospatial map is derived from the Landsat satellite images on the Google Earth Engine. We use the version with 30 meter resolution identified for the year 2022. For each original cell, we identify it as inhabitable if it is not cropland or impervious, which consequently includes all forest, shrub, grassland, water, snow and ice, barren, and wetland cells. The cells are converted to 500-meter cells used in the NTL geospatial data. For each converted cell, we identify it as inhabitable if all associated original cells are inhabitable.

A.3 Land Transaction Data of China

China's land transaction data are processed from Land China (www.landchina.com).[24] Each land transaction is identified by an Electronic Identification number (EID). The sample period ranges from 2000 to 2020.

Geolocation. We convert textual addresses into geographic coordinates using a commercial geocoding API (Amap). The input includes address, city, and province, and the output provides latitude and longitude. To ensure accuracy, we exclude observations with imprecise matches based on address resolution criteria.

For each land transaction, the dataset records the city, the address, the source of the land, the area, the financial amount of the transaction, the upper and lower bounds of the contracted floor-area ratio, the signing date of the contract, and the transacted party (usually a person or a firm). The API we use is Amap. For each observation, the input is the textual address, the city, and the province. The output is longitude, latitude, and the implied textual address. To exclude excessively rough results, we filter out outputs with textual addresses ending with a city or county name or being less than 16 characters.

Matching with NTL. Each land parcel is matched to the corresponding NTL grid cell based on geographic coordinates. Parcel-level NTL is then used as a proxy for construction activity.

To match each land transaction with a listed firm, we identify the best match from the name of the transacted party, searching for the name of the potential parent listed firm of the transacted party. For each transaction, we firstly try to directly match the transacted party with a listed firm according to the name of the transacted party. If we do not find a potential match, we manually expand the searching scope to subsidiaries of each listed firm, including those not directly identified from their names, using equity relationship in TianYanCha.[25] In this case, if the name of a transacted party matches a subsidiary firm, we match the transaction with the parent listed firm corresponding to the subsidiary firm. Currently, matches are available for all transactions from 2007 to 2015 and from 2017 to 2020. The summary statistics of the land transaction data are in Table A.3.

[23]The tif file is publicly available at: https://zenodo.org/records/8176941.

[24]We thank Xiaoyu Zhang for sharing the processed data, including matching transactions to list firms and aggregating them to city level.

[25]Founded in October 2014, TianYanCha is a website under Beijing Jindi Technology Co., Ltd.. It allows users to search for various types of information about companies in mainland China.

Table A.3: Summary Statistics: Land Transaction

	N	Mean	SD	Min	Max
Year	55090	2013.08	3.66	2007.00	2020.00
Month	55090	6.92	3.47	1.00	12.00
Day	55090	16.69	8.79	1.00	31.00
Area	55090	5.42	14.03	0.0003	1056.60
Revenue	55090	13166.19	48338.77	0.0001	3707364.00

Notes: The unit of area is hectare. The unit of revenue is 10,000 Yuan.

To aggregate the data to city level, we add the total area or revenue of all the transactions occurred within each city.

A.4 Built-up Area Classification

We classify city areas into (i) city centers, (ii) suburbs, and (iii) non-built-up areas using historical satellite-based built-up boundaries (Jiang et al., 2022).

City centers are defined as areas built up by 1990, suburbs as areas built up between 1990 and 2010, and non-built-up areas as the remaining regions excluding uninhabitable land.

Validation. We validate this classification by comparing it to official urbanization measures and by manually inspecting major cities (e.g., Beijing, Shanghai, Guangzhou). The classification closely matches conventional definitions of urban cores and expansion zones.

Robustness. Results are robust to alternative cutoff years (e.g., using 2015 instead of 2010).

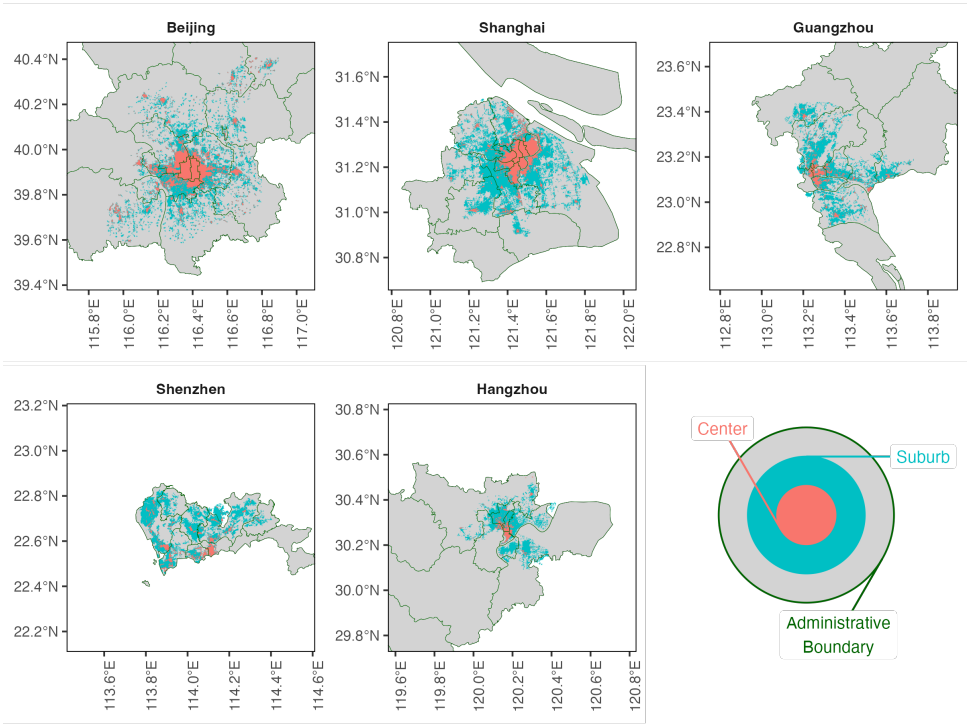

Figure A.3: Built-up Areas of Selected Cities

Notes: The boundaries of the built-up areas are identified up to 2010.

A.5 Firm-level and Bond Issuance Data

We use bond issuance data from Huang et al. (2024), which provide detailed information on issuance amounts, maturities, and currency denomination.[26] Each bond issuance is identified by an unique identification number. The sample period ranges from 2000 to 2015. For each bond issuance, the dataset records the issuer's name, the issuer's parent firm's name (if diffrent from the issuer), the matched listed firm (through stock market code), the firm's industry, the pricing date, the maturity date, the currency of the bond, and the value of the bond. It also provides information such as bond rating at issuance, current bond rating, whether the bond is of investment grade, yield to maturity, and the interest rate of the U.S. and China on the bond pricing date.

We identify whether the issuance is domestic or foreign based on the currency of the bond. If the currency of the bond is Chinese Yuan (CNY), we classify the record as domestic. Otherwise, we classify it as foreign. In this study, we focus on the records matched to a listed real estate firm. For such records, 94.14 percent of the classified foreign issuance are denominated in U.S. dollars (USD). Therefore, the U.S. interest rate can be used as a good measure of the reference bond issuance rate. The summary statistics of the land transaction data are in Table A.4.

[26]We thank Yi Huang for sharing the data.

Table A.4: Summary Statistics: Bond Issue

	N	Mean	SD	Min	Max
Pricing year	19354	2012.79	2.30	2000.00	2015.00
Pricing month	19354	6.67	3.33	1.00	12.00
Pricing day	19354	16.57	8.15	1.00	31.00
Maturing year	19354	2016.88	3.79	2003.00	2075.00
Maturing month	19354	6.59	3.35	1.00	12.00
Maturing day	19354	17.55	8.22	1.00	31.00
Total face value	19354	493.05	1791.02	0.08	161122.58

Notes: The unit of total face value is 1 million Yuan.

The operation information of listed firms in China is from China Stock Market Accounting Research (CSMAR). It contains the quarterly financial reporting information of all listed firms in China's equity market from 2007 to 2023. Each listed firm is identified by the stock quote code. Key information we use includes the industry of the firm as classified by CSRC, balance sheet indicators (assets, liabilities, accounts receivable, accounts payable, pre-sale revenue, short-term loan, long-term loan, book value of illiquid liability maturing within one year, bond payable), earning indicators (revenue, profit) and cashflow indicators (cash balance at the beginning and the end of the period).

A.6 Three-Red-Line Policy

The "three red lines" policy was introduced in August 2020 to impose leverage constraints on real estate developers.

The policy defines three thresholds: (i) liability-to-asset ratio (excluding presales) 0.7, (ii) net debt-to-equity ratio 1, (iii) cash-to-short-term debt ratio 1.

Firms violating any threshold are classified as constrained.

Treatment definition. We classify firms as treated if they violate at least one threshold in the quarter prior to policy implementation (2020Q2).

This classification generates cross-sectional variation in financing constraints used in the empirical analysis.

A.7 City-Level Exposure Measure

To study aggregate implications, we construct a city-level exposure measure capturing the extent to which land transactions are associated with financially constrained firms.

Construction. For each land transaction, we assign the financial characteristics of the associated firm. We then aggregate these characteristics at the city level using transaction-level weights (based on land revenue or area).

Bad deal index. We define the "bad deal index" as the interaction between land transaction activity and firm-level financial stress.

Controls. City-level controls include population, housing inventory measures, and real estate investment intensity.

Robustness. Results are robust to alternative weighting schemes and definitions.

A.8 Other Data

A.8.1 National Accounts

To associate variations in NTL with changes in economic activities, we need to obtain GDP and other national account indicators and adjust the NTL data to the same frequency. Two datasets are used for this purpose: the city-level annual panel in China and the country-level annual panel. We obtain the city-level national accounts of China from statistical yearbooks, which are published annually by the NBSC, and use data from 2012 to 2023. Indicators we use include total GDP, GDP in the primary, secondary, and tertiary sectors, import, and export.[27] Then, we get country-level national accounts from the World Development Indicator (WDI) of the World Bank and associate them with country-level NTL series from the Light pollution statistics. [28] We use data from 2012 to 2023 in line with the main panel.

A.8.2 Financial Data of China

We use China's financial market data, including interest rates, stock market indices, and exchange rates. They are at daily frequency, and we use full sample starting from 1990s. Interest rates we use include R007 (7-day interbank repo rate with collaterals) and SHIBOR (Shanghai Interbank Offering Rate). Stock market indices we use include SSE (Shanghai Stock Exchange) indices (Composite, Industrial, Real Estate, Infrastructure, Financial, SSE 180). Exchange rates we use include the exchange rate of USD to CNY.

A.8.3 Time Series Data of China at City Level

Most of the time series data we use are from CEIC, a comprehensive database for aggregated economic indicators. We use city-level indicators at annual frequency. We use the full sample starting from as early as 1990s. We also use some data from NBSC.

Annual series we use include urbanization indicators (urban constructed rate, urban area, urban area percentage, population urbanization percentage) and population From CEIC, we use real estate investment, land transaction data (transaction area and revenue), and floor space sold and waiting for sale.

[27] Import and export are available until 2021.

[28] The country-level NTL data here are from the Light pollution map, but they are derived from the same source as our main NTL series.

A.8.4 Time Series Data of the US

Data of the U.S. economy are from the FRED database provided by the Federal Reserve Bank (Fed) of St. Louis. We use industrial production data at monthly frequency (INDPRO).

Corresponding to the U.S. MPs series, we also adopt the U.S. news shocks (including shocks on GDP, CPI, PPI, employment, retail sales). A shock is the difference of realized and ex-ante expected values. The consensus expectations are available from the widely used survey by Action Economics, the successor to Money Market Services. We use the "advance" GDP release, headline CPI and PPI inflation, and non-farm payrolls from the employment report. The retail sales are the total sales including automobiles. This data is obtained from Lakdawala et al. (2021).

A.8.5 Weather

Like the NTL data, weather data are also available daily. Weather potentially impacts NTL through channels irrelevant to productivity. Therefore, we control for daily weather conditions as a robustness check. The weather series can also be used as a placebo test, as their changes are supposed to be relatively irrelevant to the MPs. The data source is the Global Surface Summary of the Day (GSOD) from the National Oceanic and Atmospheric Administration (NOAA).[29] We use the average daily temperature, visibility, and wind speed data since 2014 in the study.

Appendix B Validation of Nighttime Light as a Measure of Economic Activity

This appendix provides validation for the use of nighttime light (NTL) as a proxy for real economic activity, with a focus on the construction margin studied in the paper. We present two pieces of evidence. First, we show that NTL is strongly correlated with standard measures of economic activity. Second, we provide evidence that parcel-level NTL captures construction-related activity.

B.1 Cross-city Validation

We begin by validating NTL as a proxy for aggregate economic activity. Following the literature, we relate changes in NTL to changes in GDP at the city level. Figure B.1 shows such associations at annual frequency and the city level.

[29]The data are publicly accessible at: https://www.ncei.noaa.gov/access/metadata/landing-page/bin/iso?id=gov.noaa.ncdc:C00516.

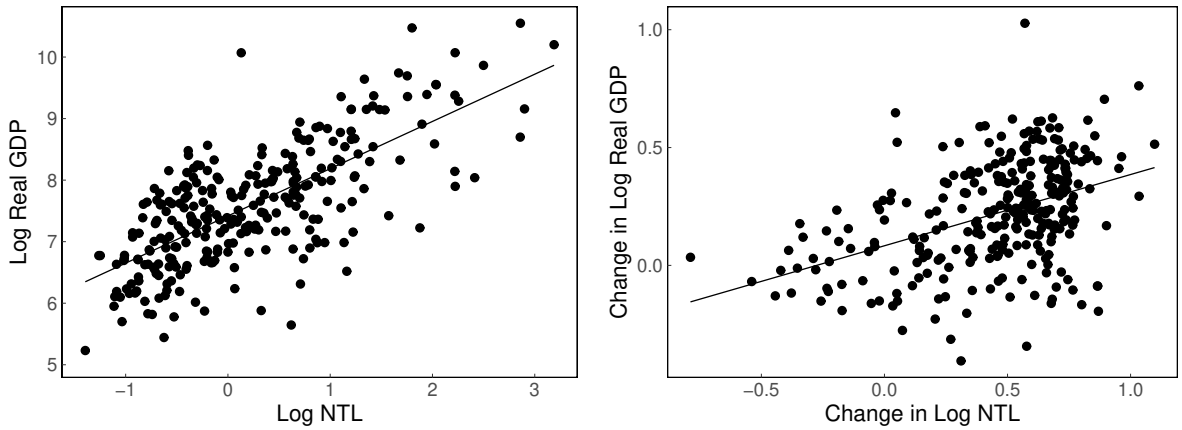

Figure B.1: NTL and GDP by City

Notes: Log NTL is converted to the corresponding frequency of the national account indicators in each plot. Log NTL is the logged value of the average NTL across every day in the converted periods. For each day, NTL is the average value of all cells in each city. The left graph shows the data in 2019. The right graph shows the changes from 2012 to 2019.

Using the annual panel data with NTL and different indicators from the national accounts, we apply the following regression equation.

$$y_{i,t} = \beta_0 l_{i,t} + \gamma_i + \tau_t + u_{i,t} \tag{B.1}$$

Here y is an output indicator (e.g., log GDP), and l is the log NTL. i and t are identifiers for city and year, respectively. We use NTL in the last year as the IV of the current NTL following J. Kim et al. (2022) and Chor and Li (2024). We also control for two-way fixed effects. When both y and l are in log forms, β_0 is the elasticity of output on NTL. The regression results of overall GDP and GDP by sector on NTL are in Table B.1.

The elasticity for aggregate GDP is about 0.49 (excluding Covid period), consistent with previous literature. Further looking at the elasticity by sector, the primary sector (agriculture) GDP does not correlate with NTL (Gibson et al., 2024), as agriculture activities mainly occur during the days. Both secondary (manufacturing and construction) and tertiary (service) sectors' GDP significantly and substantially correlate with NTL. Table B.2 implies the significant elasticity across periods. Therefore, the fluctuation in NTL reflects changes in economic output.

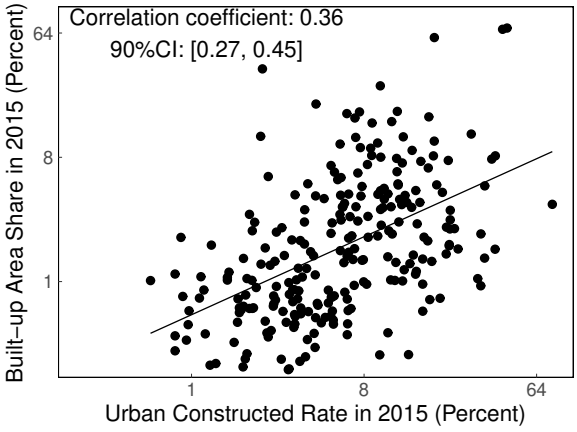

Figure B.2: Built-up Area Share and Urban Constructed Rate by City

Notes: For each city, the built-up area share is calculated as the ratio of the total number of NTL cells of the built-up area of the city over the total number of NTL cells of the city.

B.2 Cross-country Validation

Next, we run the same regression in Equation B.1 at the country level using the cross-country national accounts, and the results are in Table B.3. In line with previous literature (Bickenbach et al., 2016; Henderson et al., 2012; Martínez, 2022), NTL has a higher correlation with GDP for emerging economies. Intuitively, several channels of GDP growth reflected on NTL mostly apply to emerging economies, including urbanization and night shifts in the manufacturing sector.

The evidence in this appendix supports the use of nighttime light as a proxy for real economic activity, particularly for construction-related investment. NTL is strongly correlated with aggregate output. These properties make it a suitable measure for studying the real effects of monetary policy at high frequency and fine spatial resolution.

Table B.1: Regression of GDP on NTL: Sector

Dependent Variable:	Log GDP			
Sector:	All	Primary	Secondary	Tertiary
Model:	(1)	(2)	(3)	(4)
Variables (Second stage)				
Log NTL	0.4900***	0.1053	0.8280***	0.4938***
	(0.0793)	(0.0708)	(0.1254)	(0.0866)
Fixed-effects				
City	Yes	Yes	Yes	Yes
Year	Yes	Yes	Yes	Yes
Fit statistics				
N	2,527	2,293	2,293	2,293
R^2	0.9873	0.9834	0.9676	0.9878
F-test	3,161.7	2,128.7	1,115.1	3,021.7

Notes: The COVID period from years 2020 to 2022 (both included) are excluded. The instrumental variable of the log nighttime light is the same indicator in the previous period. The first-stage regression coefficient is 0.6867 (s.e.: 0.0220). Significance levels are based on Clustered (Region) standard-errors. Significance Codes: ***: 0.01, **: 0.05, *: 0.1.

Table B.2: Regression of GDP on NTL: Periods

Dependent Variable:	Log GDP			
Period:	All	Exclude COVID	2012-2016	2017-2023
Model:	(1)	(2)	(3)	(4)
Variables (Second stage)				
Log NTL	0.2559***	0.4900***	0.9435***	0.2802***
	(0.0583)	(0.0793)	(0.1124)	(0.0844)
Variables (First stage)				
Log NTL (Lag 1)	0.7234***	0.6867***	0.5188***	0.5060***
	(0.0135)	(0.0220)	(0.0317)	(0.0627)
Fixed-effects				
City	Yes	Yes	Yes	Yes
Year	Yes	Yes	Yes	Yes
Fit statistics				
N	3,475	2,527	1,580	947
R^2	0.9861	0.9873	0.9936	0.9953
F-test	2,041.7	3,161.7	10,708.6	21,922.0

Notes: The COVID period includes years 2020 to 2022 (both included). The subperiod 2017 to 2023 also excludes the COVID period. Significance levels are based on Clustered (Region) standard-errors. Significance Codes: ***: 0.01, **: 0.05, *: 0.1.

Table B.3: Regression of GDP on NTL: Countries by Income Group

Dependent Variable:	Log GDP		
Group:	All	Higher income	Lower income
Model:	(1)	(2)	(3)
Variables (Second stage)			
Log NTL	0.1420***	0.0403	0.1277**
	(0.0444)	(0.0717)	(0.0511)
Variables (First stage)			
Log NTL (Lag 1)	0.7791***	0.6812***	0.7687***
	(0.0407)	(0.0460)	(0.0588)
Fixed-effects			
Country	Yes	Yes	Yes
Year	Yes	Yes	Yes
Fit statistics			
N	1,997	984	1,003
R^2	0.9990	0.9992	0.9986
F-test	19,166.4	11,904.7	7,313.8

Notes: The economies are classified into higher income and lower income economics by comparing their GDP per capita in 2012 with the median of all the economies in the sample. GDP value used is the constant GDP in 2015 US dollars (World Bank API indicator code: NY.GDP.MKTP.KD). Significance levels are based on Clustered (Region) standard-errors. Significance Codes: ***: 0.01, **: 0.05, *: 0.1.

Appendix C Robustness of Baseline Results

This appendix reports robustness checks for the main empirical findings. We focus on four dimensions: (i) alternative measures of monetary policy shocks, (ii) inference and estimation choices, (iii) potential confounding factors, and (iv) alternative sample definitions. Across all specifications, the main results remain qualitatively unchanged.

C.1 Alternative Measurements

We verify that the results are robust to alternative measures of U.S. monetary policy shocks and NTL.

First, we use the conventional monetary shock series constructed by Acosta (2022). Second, concerning the measurement error induced by recorded light in the human-less areas, we remove the mountains and other uninhabitable areas.

Figure C.1 shows that the impulse responses are quantitatively similar across these

measures. In all cases, U.S. monetary tightening leads to a decline in nighttime light (NTL). These results indicate that the findings are not driven by a particular choice of measurements.[30]

C.2 Inference and Estimation

We examine the robustness of inference to alternative estimation choices.

First, To exclude the noises from low-frequency factors, we add year-quarter fixed effects (FE) to our baseline specification. Second, we compute confidence intervals using a bootstrap procedure to account for serial correlation. Third, we vary lag lengths in the local projection specification.

Figure C.1 shows that the results are stable across these alternatives. In particular, the magnitude and timing of the responses remain largely unchanged.

C.3 Controlling for Confounding Factors

We assess whether the results are driven by other factors that may co-move with U.S. monetary policy.

First, we control for U.S. news shocks[31] or U.S. industrial production. Second, we include indicators of U.S.–China trade tensions constructed by Rogers et al. (2024) to account for contemporaneous geopolitical shocks. Third, we control China's local weather conditions, including temperature and precipitation, which may affect nighttime light independently of economic activity.

Figure C.2 shows that the estimated responses remain similar after including these controls, suggesting that the results are not driven by omitted variables correlated with monetary policy shocks.

C.4 Alternative Sample Definitions

We examine whether the results are sensitive to sample selection.

First, we exclude observations corresponding to major holidays and extreme weather events. Second, we restrict the sample to periods without significant domestic policy interventions.

Figure C.4 shows that the results are robust across these alternative samples.

[30] We also perform a falsification test by replacing the baseline's NTL with weather indicators. As expected, we do not find any significant responses by these indicators. The results are available upon request.

[31] The macro news shocks include GDP, CPI, PPI, Employment, and Retail Sales surprises, which are the differences between the data release and the previous consensus expectations. They are obtained from the widely used survey by Action Economics, the successor to Money Market Services. We use the "advance" GDP release, headline CPI and PPI inflation, and non-farm payrolls from the employment report. The retail sales are the total sales including automobiles. The data are from Lakdawala et al. (2021).

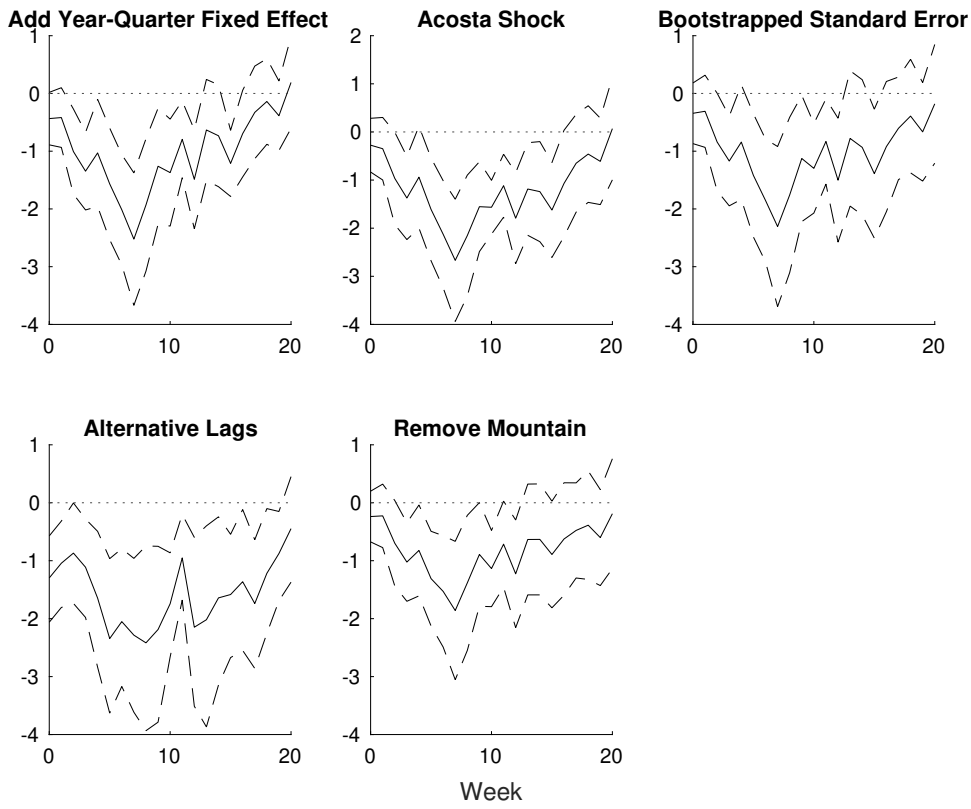

Figure C.1: Local Projection of China's NTL on U.S. MPs: Alternative Measurements and Specifications

Notes: MPs is aggregated to the weekly frequencies consistent with the dependent variable.

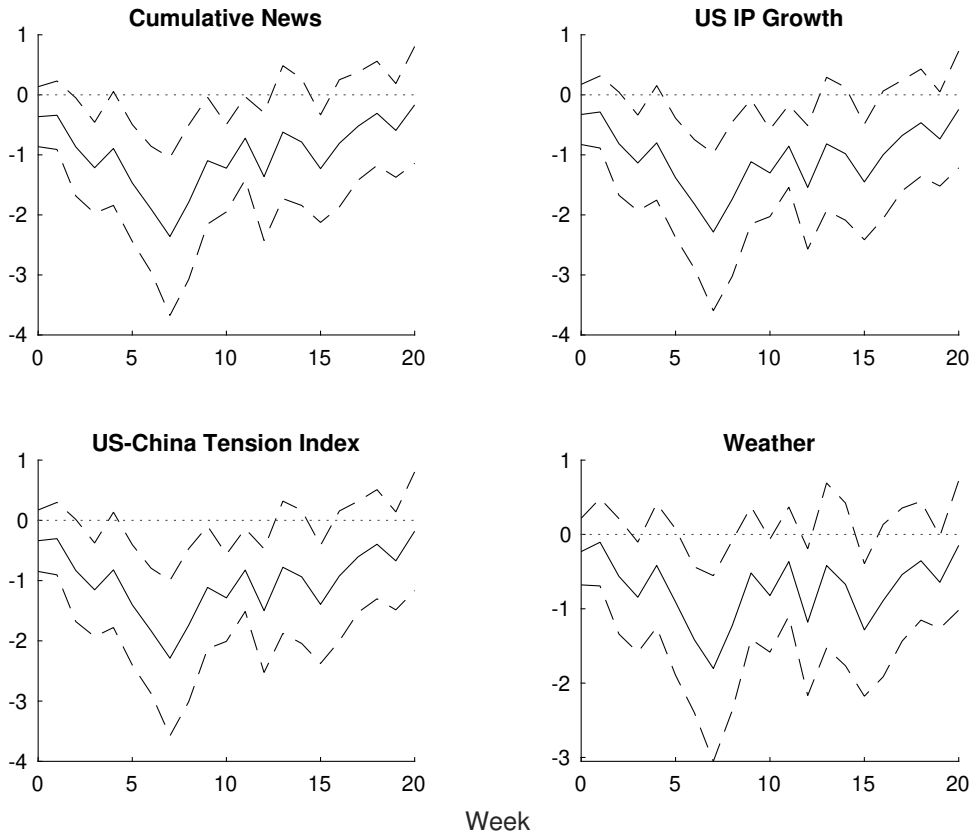

Figure C.2: Local Projection of NTL on U.S. MPs: Adding Controls

Notes: For each graph, the title is the control added. For news, the control variables include cumulative GDP, CPI, PPI, employment, and retail sales news shocks. Each news shock is cumulative with a 60-day window before FOMC announcements. For U.S. Industrial Production growth, Industrial Production is from a monthly series. Its values attached to each week are the period-to-period changes in the last period corresponding to the quarter and month of the week. For weather, control variables include average temperature, visibility, and wind speed. MPs is aggregated to the weekly frequencies consistent with the dependent variable. The number of lags of the dependent variable (Q) and the shocks (M_1 and M_2) are selected by the AIC criteria for up to 4 periods. The dashed bands are the 90 percent confidence intervals generated based on the Newey-West standard errors.

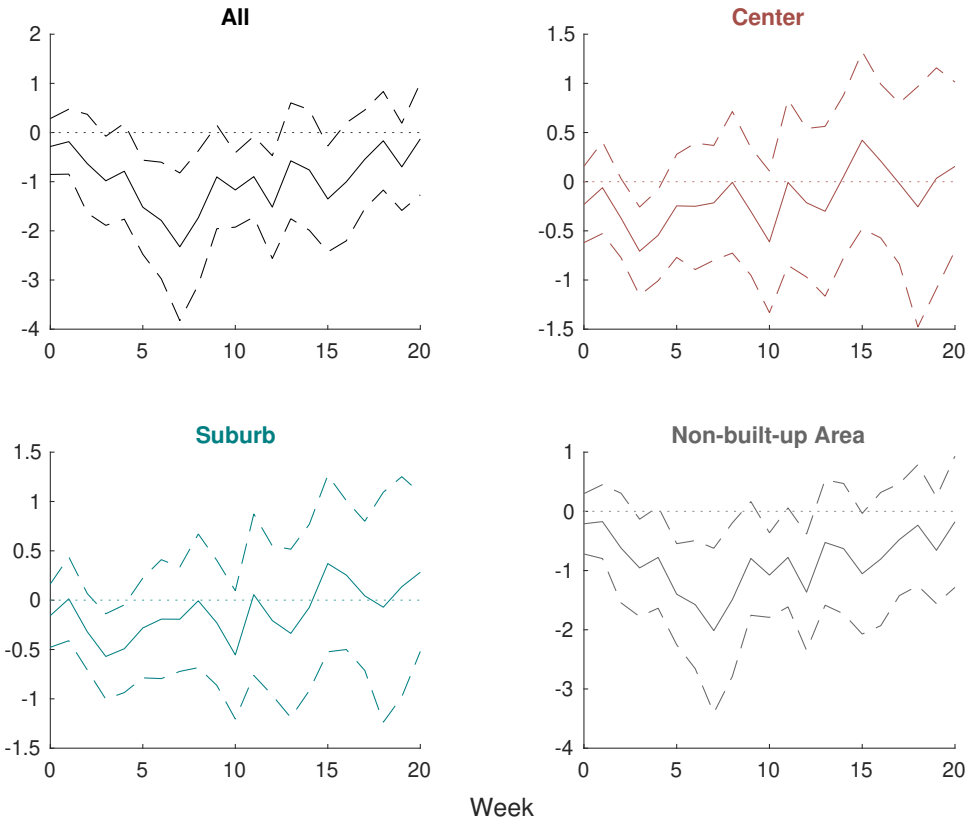

Figure C.3: Local Projection of NTL on U.S. MPs: City Areas, Identified Built-up Area in 2015

Notes: MPs is aggregated to the weekly frequencies consistent with the dependent variable. The dashed bands are the 90 percent confidence intervals generated based on the Newey-West standard errors.

C.5 Seasonal Validation of the Construction Channel

Since the intensity of construction activities might be influenced by whether conditions, another test of the construction channel is to compare the differential responses of NTLs to U.S. MP shocks between summer and winter. For example, in some northern parts of China, construction fields do not operate in winter due to extremely low temperature, and NTL from construction activities should respond less to the U.S. tightening than during the summer. This contrasts to the south region, where the intensity of construction activities should be less affected by seasons. To test this, we split our sample into cities in the north and south regions of China when aggregating NTL at the city level.[32] We further divide the sample period into the summer period and the winter period. The summer period is from April to September. The winter period is October to March in the next year.

As shown in Figure C.4, for the northern region, the NTL responses to U.S. MPs in the summer are significant, while the response in the winter is statistically indifferent from zero. In contrast, for the southern region, the difference across seasons is relatively

[32]The division here follows the official definition of NBSC.

weaker than that in the north (see Figure C.5).[33]

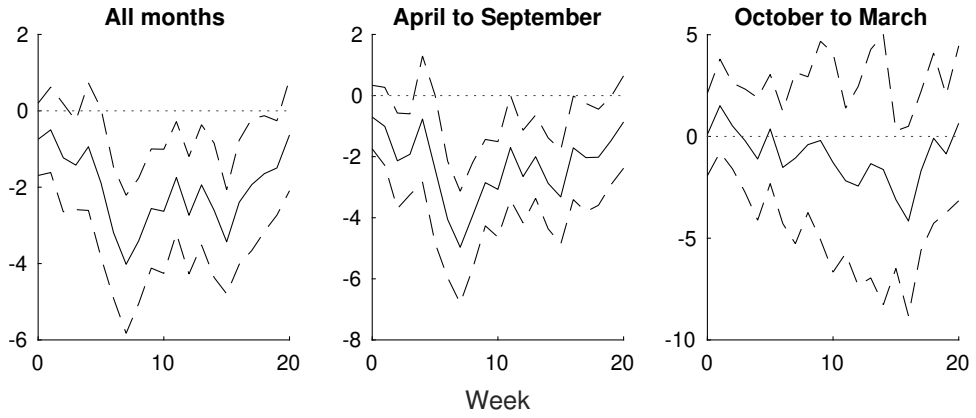

Figure C.4: Local Projection of NTL on U.S. MPs: North, Summer vs Winter Periods

Notes: MPs is aggregated to the weekly frequencies consistent with the dependent variable. The number of lags of the dependent variable (Q) and the shock (M) are selected by the AIC criteria for up to 4 periods. The dashed bands are the 90 percent confidence intervals generated based on the Newey-West standard errors.

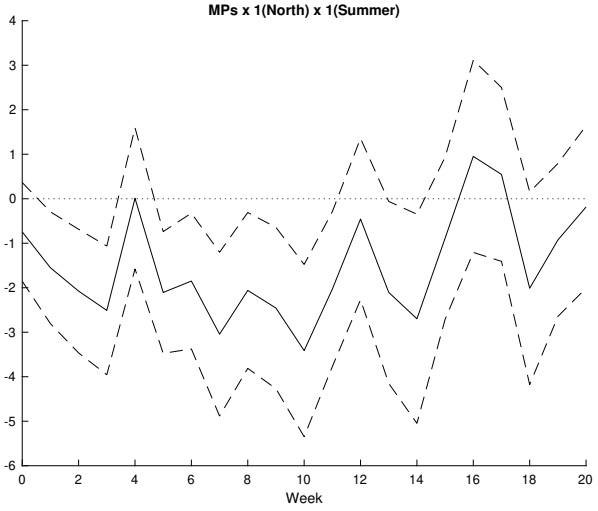

Figure C.5: Local Projection of NTL on U.S. MPs: North and South, Summer versus Winter

Notes: MPs is aggregated to the weekly frequencies consistent with the dependent variable. The dashed bands are the 90 percent confidence intervals generated based on the Newey-West standard errors.

[33]To compare the different response seasonality between the north and the south, we apply a triple interaction identification: $y_{i,t+h} - y_{i,t-1} = \alpha_i^{(h)} + \sum_{q=1}^{4} \phi_q^{(h)} \Delta y_{i,t-q} + \beta_1^{(h)} x_t + \beta_2^{(h)} \mathbb{1}(\text{North}_i) + \beta_3^{(h)} x_t \mathbb{1}(\text{North}_i) + \beta_4^{(h)} x_t \mathbb{1}(\text{Summer}_t) + \beta_5^{(h)} \mathbb{1}(\text{North}_i)\mathbb{1}(\text{Summer}_t) + \beta_6^{(h)} x_t \mathbb{1}(\text{North}_i)\mathbb{1}(\text{Summer}_t) + u_{i,t+h|t}$, where i is the province. We expect β_6 to be negative.

Appendix D More Evidence on Channel

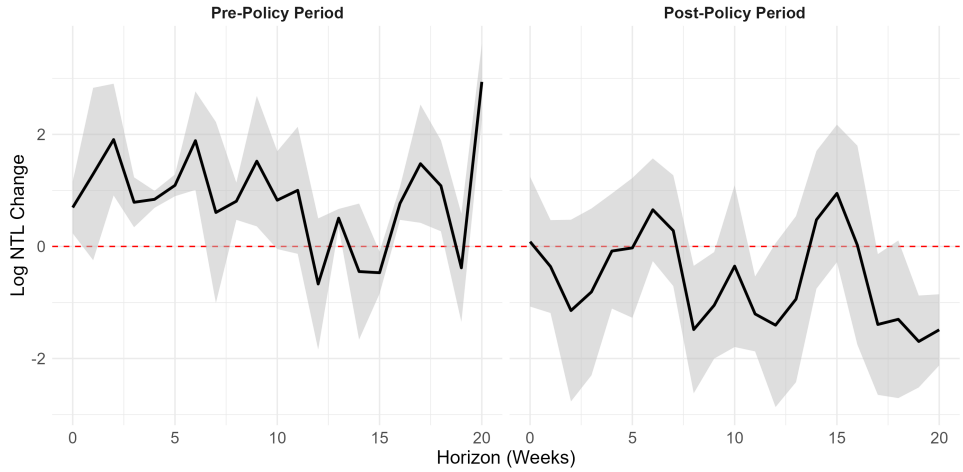

Figure D.1: Response of NTL to US MPs: Three Red Line Policy, Pre versus Post Policy Period

Notes: This graph displays the heterogeneous responses across firms in different periods. The sample period is a 2-year window (2020–2021) centered around the policy implementation date of August 20, 2020. The specification is: $y_{i,t+h} - y_{i,t-1} = \alpha_i^{(h)} + \alpha_t^{(h)} + \sum_{q=1}^{4} \phi_q^{(h)} \Delta y_{i,t-q} + \beta_1^{(h)} x_t Cross_i^j + \beta_2^{(h)} Cross_i^j + \gamma^{(h)} W_{i,t-L} + u_{i,t+h|t}$, where $j = 3$, denoting the third line, short-term debt constraint. We estimate this specification for pre-policy and post-policy period separately. The coefficients of $\beta_1^{(h)}$ are plotted. The shaded areas represent the 90 percent confidence intervals, constructed using two-way clustered standard errors at the firm and week levels.

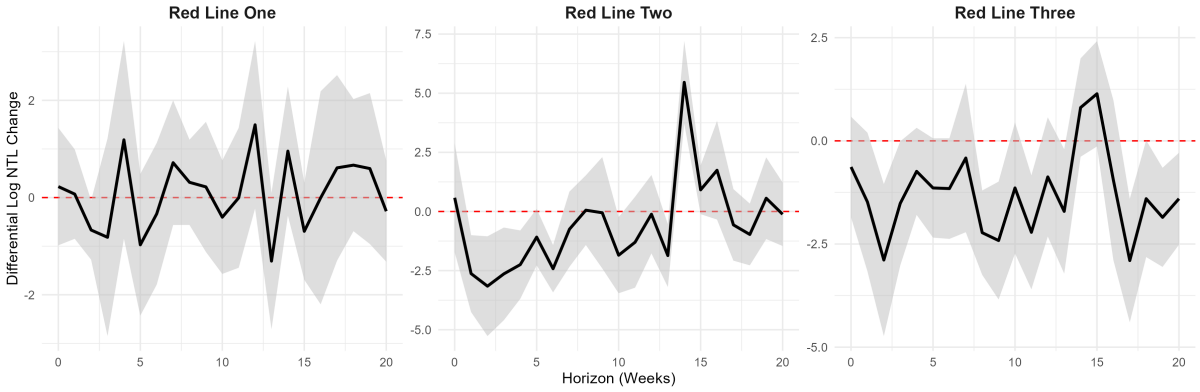

Figure D.2: Response of NTL in Transacted Land to U.S. MPs: Before and After the Three Red Line Policy Implementation, Red Line Crossed Firms versus Non-Crossed Firms

Notes: This graph displays the heterogeneous responses across firms before and after the implementation of the "three red line" policy. The sample period is from 2020 to 2021 with a 2-year window around the policy implementation date, August 20, 2020. The specification is in Equation 3. Each subfigure plots the corresponding coefficient of the triple interaction term $\beta_j^{(h)}$, $j = 1,\ 2,\ 3$, denoting liability-to-asset constraint, net gearing constraint, and short-term debt constraint, respectively. The shaded areas represent the 90 percent confidence intervals, constructed using two-way clustered standard errors at the firm and week levels.

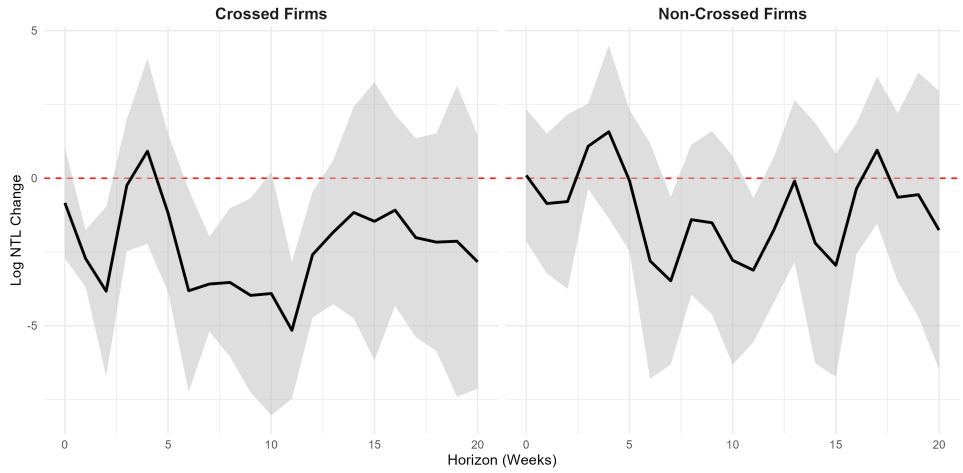

Figure D.3: Response of NTL U.S. MPs: Three Red Line Policy, Short Debt Constrained Firms versus Unconstrained Firms

Notes: this graph displays the heterogenous responses across policy periods for each group of firms. The sample period is a 2-year window (2020–2021) centered around the policy implementation date of August 20, 2020. The specification is: $y_{i,t+h} - y_{i,t-1} = \alpha_i^{(h)} + \sum_{q=1}^{4} \phi_q^{(h)} \Delta y_{i,t-q} + \beta_1^{(h)} x_t + \beta_2^{(h)} x_t Policy_t + \beta_3^{(h)} Policy_t + \gamma^{(h)} W_{i,t-L} + u_{i,t+h|t}$. We estimate this specification separately for firms that crossed the third red line, short-term debt constraint, and those that did not. The coefficients of $\beta_2^{(h)}$ are plotted. The shaded areas represent the 90 percent confidence intervals, constructed using two-way clustered standard errors at the firm and week levels.

Appendix E Shapley Decomposition

To complement the coefficient-based relative share decomposition, we employ an alternative approach based on the explanatory power (Within R^2) of each debt component. This method provides an objective measure of how much variance in the financing channel is driven by each type of debt.

E.1 Methodology

We isolate the contribution of the three interaction terms ($MPS_t \times I(FB)$, $MPS_t \times I(DB)$, and $MPS_t \times I(DL)$) to the model's explanatory power. Since these components may be correlated, calculating their individual contributions to the R^2 depends on the order they are added to the regression.

To resolve this, we use the **Shapley Value Decomposition** of the Within R^2, an axiomatic approach grounded in cooperative game theory (Shapley, 1953; Nobel Memorial Prize in Economic Sciences) and established as the gold standard in the econometric literature for unambiguously attributing the goodness-of-fit (R^2) among correlated explanatory variables (Shorrocks, 1982; Shorrocks, 2013; Lee et al., 2026).

Let $K = \{FB, DB, DL\}$ be the set of the three interaction terms, and $R_h^2(S)$ be the Within R^2 of the model at horizon h that includes a subset $S \subseteq K$ of these terms (along with all baseline variables, fixed effects, and lagged controls). The Shapley value (average marginal contribution) for a component $j \in K$ at horizon h is calculated as:

$$Shapley_{j,h} = \sum_{S \subseteq K \setminus \{j\}} \frac{|S|!\,(|K| - |S| - 1)!}{|K|!} \Big(R_h^2(S \cup \{j\}) - R_h^2(S) \Big)$$

Deconstructing the Formula and Intuition:

In a regression model, when variables (like the three debt components) are correlated, the sequence in which they are added affects their marginal contribution to the model's explanatory power (R^2). The Shapley value resolves this multicollinearity issue by calculating the weighted average of a variable's marginal contribution across all possible permutations of adding variables.

- j: The specific variable whose contribution is being calculated (e.g., $j = FB$).
- K: The set of all candidate variables to be decomposed. Here, $|K| = 3$ for $\{FB, DB, DL\}$.
- S: A subset of variables already included in the model *before* adding variable j. If $j = FB$, S could be $\emptyset$, $\{DB\}$, $\{DL\}$, or $\{DB, DL\}$.
- $R_h^2(S \cup \{j\}) - R_h^2(S)$: The **Marginal Contribution**—how much the R^2 increases when j is added to the model that already contains the variables in S.
- $\frac{|S|!\,(|K|-|S|-1)!}{|K|!}$: The probability weight ensuring the marginal contribution of j is fairly averaged across all $3! = 6$ possible sequential orderings. For example, if $j = FB$:
  - FB is added first ($S = \emptyset$) in 2 permutations. Weight: $2/6 = 1/3$.
  - FB is added second after DB ($S = \{DB\}$) in 1 permutation. Weight: $1/6$.
  - FB is added second after DL ($S = \{DL\}$) in 1 permutation. Weight: $1/6$.
  - FB is added last ($S = \{DB, DL\}$) in 2 permutations. Weight: $2/6 = 1/3$.

By summing these weighted marginal contributions, the Shapley value provides a strictly fair decomposition where the sum of individual contributions perfectly equals the total R^2 added by the joint inclusion of all variables:

$$\Delta R_h^2 = R_h^2(K) - R_h^2(\emptyset) = \sum_{j \in K} Shapley_{j,h}.$$

This completely purges any distortions caused by multicollinearity among the financing channels.

The relative contribution share of component j is defined as its time-averaged Shapley value divided by the time-averaged total added R^2:

$$Share_j = \frac{\frac{1}{21}\sum_{h=0}^{20} Shapley_{j,h}}{\frac{1}{21}\sum_{h=0}^{20} \Delta R_h^2}$$

E.2 Regression Specification for R^2 Decomposition

To compute the Within $R_h^2(S)$ for any given subset S, we estimate a series of restricted Local Projections models corresponding to the baseline specification (Section 2.2). Because there are three candidate interaction terms ($|K| = 3$), the decomposition requires estimating $2^3 = 8$ distinct regressions for each horizon h.

Let the three interaction terms of interest be defined as:

- $X_{i,t}^{FB} = MPS_t \times I(FB)_{i,t-1}$
- $X_{i,t}^{DB} = MPS_t \times I(DB)_{i,t-1}$
- $X_{i,t}^{DL} = MPS_t \times I(DL)_{i,t-1}$

We define the set of base control variables ($Controls_{i,t}$) held constant across all 8 sub-regressions:

$$Controls_{i,t} = \gamma_h MPS_t + \delta_h I(FB)_{i,t-1} + \zeta_h I(DB)_{i,t-1} + \eta_h I(DL)_{i,t-1} + \sum_{l=1}^{4} \rho_{h,l} \Delta \ln(NTL_{i,t-l}) + \alpha_i$$

Note: $Controls_{i,t}$ does not include additional time-varying firm characteristics. It strictly controls for the main effects of the debt indicators, the baseline monetary policy shock, the 4 lags of the dependent variable, and firm fixed effects (α_i).

The 8 sub-regressions estimated at each horizon h are:

1. **Zero interactions ($S = \emptyset$):** $\Delta \ln(NTL_{i,t+h}) = Controls_{i,t} + \epsilon_{i,t+h}$
2. **One interaction ($|S| = 1$):** 3 regressions, e.g. $\Delta \ln(NTL_{i,t+h}) = \beta_h^{(FB)} X_{i,t}^{FB} + Controls_{i,t} + \epsilon_{i,t+h}$
3. **Two interactions ($|S| = 2$):** 3 regressions, e.g. $\Delta \ln(NTL_{i,t+h}) = \beta_h^{(FB)} X_{i,t}^{FB} + \beta_h^{(DB)} X_{i,t}^{DB} + Controls_{i,t} + \epsilon_{i,t+h}$
4. **All three interactions ($S = K$):** The full unrestricted model (Section 2.2).

The difference in the Within R^2 between any two nested models yields the marginal contribution $\left(R_h^2(S \cup \{FB\}) - R_h^2(S)\right)$ used in the Shapley formula.

Appendix F Alternative Monetary Policy Shocks and Channels

This section presents additional evidence on the international spillover effects of monetary policy, focusing on the role of policy types, source countries, and alternative transmission channels.

F.1 Conventional versus Unconventional Monetary Policy

We first compare the effects of conventional and unconventional U.S. monetary policy. Following Jarociński, 2024, we decompose monetary policy shocks into target rate shocks, forward guidance shocks, large-scale asset purchase (LSAP) shocks, and information shocks. We test the impacts of target rate shock (close to the federal fund rate shock in the baseline), forward guidance shock (or called Odyssean forward guidance, close to the path shock in Gürkaynak and Sack, 2005), Large-scale asset purchase shock (LSAP), and information shock (or called Delphic forward guidance). These shocks are decomposed by Jarociński, 2024.

The comparison is displayed in Figure E.1. It is found that only targeted FFR tightening shock has a significantly negative impact on NTL, but not forward guidance, LSAP or information shocks, which suggests that the conventional monetary policy seems to be more effective in affecting real output. These findings suggest that the transmission mechanism identified in this paper operates primarily through channels associated with short-term interest rates and borrowing costs, rather than through expectations or balance sheet expansion.

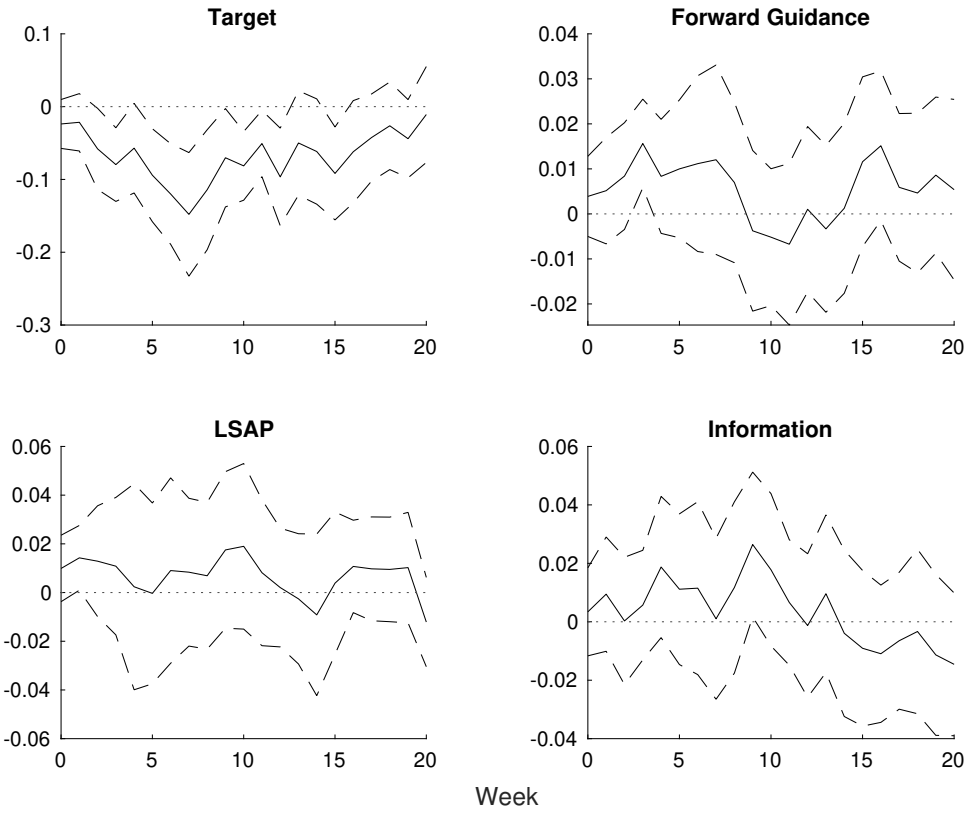

Figure E.1: Local Projection of NTL on U.S. MPs: Alternative Unconventional MPs

Notes: MPs is aggregated to the weekly frequencies consistent with the dependent variable. The number of lags of the dependent variable (Q) and the shock (M) are selected by the AIC criteria for up to 4 periods. The dashed bands are the 90 percent confidence intervals generated based on the Newey-West standard errors.

F.2 MPs of China and Other Economies

We next examine whether monetary policy shocks from other major economies than the U.S. have similar spillover effects. Using high-frequency shocks identified for the People's Bank of China (PBC), the European Central Bank (ECB), and the Bank of Japan (BOJ), we estimate their impact on China's real activity.[34] Specifically, we apply the baseline LP identification and replace U.S. MPs with the shocks by PBC, ECB, and BOJ. The IRFs are in Figure E.2.

The results show that U.S. monetary policy has the strongest and most consistent effects, while shocks from the ECB and BOJ are generally insignificant. China's own monetary policy exhibits effects similar in direction to U.S. shocks, reflecting its influence on domestic financing conditions. [35] These findings are consistent with the dominant role of the U.S. dollar in global financial markets (Gopinath et al., 2020) and the central role of U.S. monetary policy in driving the global financial cycle (Miranda-Agrippino and Rey, 2020).

[34]The PBC shock is obtained from Shieh (2024). The ECB shock is identified from Miranda-Agrippino and Nenova (2022). The BOJ shock is identified from Kubota and Shintani (2022).

[35]We also test the corresponding path shocks for each central bank, and don't find significant effects either.

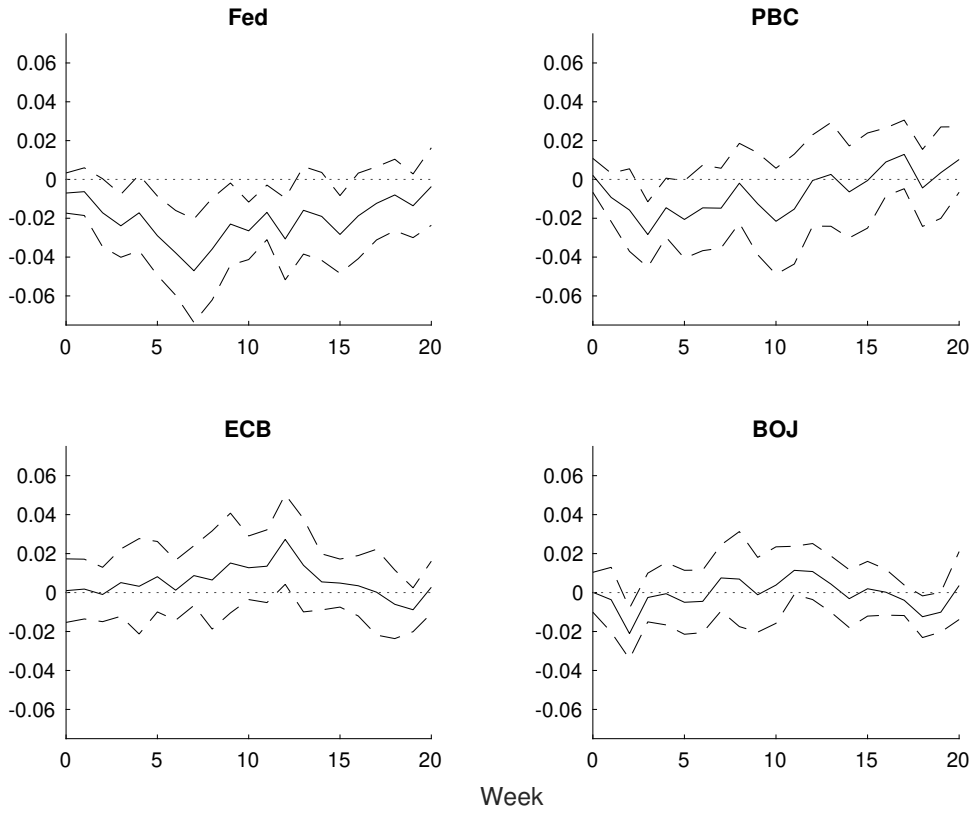

Figure E.2: Local Projection of NTL on MPs by Different Central Banks

Notes: MPs is aggregated to the weekly frequencies consistent with the dependent variable. We normalize the standard deviation of all the shocks to be 1 for the full sample so that the impacts across the shocks are more comparable. The number of lags of the dependent variable (Q) and the shock (M) are selected by the AIC criteria for up to 4 periods. The dashed bands are the 90 percent confidence intervals generated based on the Newey-West standard errors.

F.3 Trade Exposure

Finally, we examine whether trade exposure mitigates the effects of U.S. monetary tightening. A contractionary U.S. monetary shock is typically associated with a stronger U.S. dollar, which may improve the competitiveness of exporting economies.

We test this channel by interacting monetary policy shocks with city-level net export shares. The specification is the same as the urban constructed rate regression (Equation 3), except for replacing the urban constructed rate indicator with the net export share. We use net export share in the last year as the proxy for net export share to preclude endogeneity issues. The key coefficient estimate is β_2. The IRF of β_2 obtained from varying h from 0 to 10 is in Figure E.3.

The results indicate that cities with higher export exposure experience significantly smaller declines in NTL following U.S. monetary tightening. The interaction term is overall positive. In other words, although the overall negative responses are driven by the construction channel, we find that trade exposure could mitigate these adverse impacts — cities with higher trade exposure are less negatively impacted by a contractionary U.S. MPs.

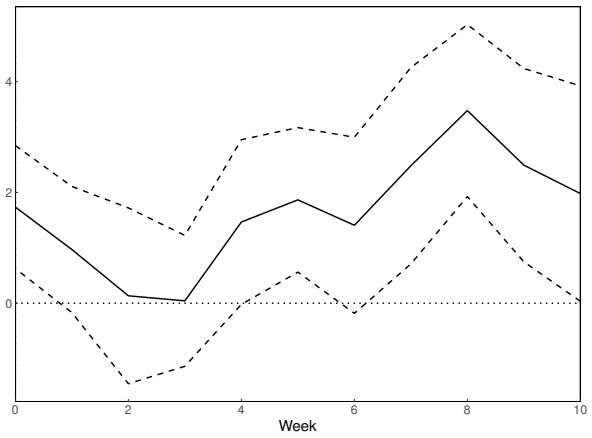

Figure E.3: NTL Response to Interaction of U.S. MPs and Trade Exposure, City level

Notes: The dashed bands are the 90 percent confidence intervals generated based on standard errors clustered to city and week.